A Scaled Bilateral Teleoperation System for Robotic-Assisted Surgery with Time Delay

Jing Guo, Chao Liu, Philippe Poignet

A Scaled Bilateral Teleoperation System for Robotic-Assisted Surgery with Time Delay

Jing Guo, Chao Liu & Philippe Poignet

Journal of Intelligent & Robotic Systems
with a special section on Unmanned Systems

ISSN 0921-0296

J Intell Robot Syst
DOI 10.1007/s10846-018-0918-1

Springer

Journal of Intelligent & Robotic Systems
https://doi.org/10.1007/s10846-018-0918-1

A Scaled Bilateral Teleoperation System for Robotic-Assisted Surgery with Time Delay

Jing Guo[1] · **Chao Liu**[2] · **Philippe Poignet**[2]

Received: 4 September 2017 / Accepted: 13 August 2018

Abstract

The master-slave teleoperated robotic systems have advanced the surgeries in the past decades. Time delay is usually caused due to the data transmission between communication channel connecting the master and slave in bilateral teleoperation, which is crucial because even small time delay could destabilize the whole teleoperation system. Motivated to solve the instability caused by time delay in bilateral teleoperation, wave variable transformation (WVT) structure has been proposed to passivate the delayed communication channel. However, conventional WVT structure provides poor velocity, position and force tracking performances which are not sufficient for surgical applications. In this paper, a new wave variable compensation (WVC) structure is proposed to improve the tracking performances with less conservative condition and comprehensive analysis to keep stable and improved tracking performance is also provided. In order to better facilitate certain surgical procedures with special requirements, e.g. robotic-assisted neurosurgery, velocity/position and force scalings are designed in the proposed structure with guaranteed system passivity, and transparency of the scaled WVC structure is also analyzed. Simulation and experimental studies were carried out to verify the performance of the proposed structure with time delay. System performance comparisons with several existing wave based bilateral teleoperation structures are also provided through simulation studies to show the improvements brought by the proposed teleoperation structure.

Keywords Robotic-assisted surgery · Time delay · Bilateral teleoperation · Wave variable · Passivity · Transparency

1 Introduction

The utilization of robotic technology in operating room has advanced the minimally invasive surgery (*MIS*) with more accurate manipulation, increased operation dexterity and enhanced visualization of the operative site. In most robotic-assisted MIS procedures, the system is designed in master-slave teleoperation way. Teleoperation has extended operator's capability to perform tasks in remote manner, and has benefited many applications such as in telesurgery [1], medical simulation [2, 3], space exploration [4], nuclear plants [5], underwater vehicles [6] and others [7]. In the scenario of robotic-assisted MIS, the surgeon sits at the master console to perform the surgical procedures by manipulating the slave robot(s) which is/are equipped with various clinical instruments, such as endoscopes, blunt and sharp dissectors, scalpels, and forceps etc. The robotic-assisted MIS has numerous advantages such as reduced trauma, shorter hospital stay time and less complication, etc. [10–14]. Despite the significant developments of robotic-assisted surgery (*RAS*), there are still many issues to be further investigated, such as haptic feedback (force and tactile) which is missing in most current surgical robotic systems. Without haptic feedback, the operation may be limited as the surgeon cannot feel accurate force applied to the operative environment [15]. As a consequence, the surgeon may exert unexpected force on the patient organs, which could cause serious safety issues for the RAS [16]. Bilateral teleoperation is introduced in RAS in order to provide force feedback to the operator [17–19].

✉ Chao Liu
liu@lirmm.fr

Jing Guo
jing.guo@gdut.edu.cn

Philippe Poignet
poignet@lirmm.fr

[1] School of Automation, Guangdong University of Technology, Guangzhou, 510006, China

[2] LIRMM, CNRS-University of Montpellier, 161 Rue Ada, Montpellier, 34095, France

Published online: 22 August 2018

In general bilateral teleoperation systems, the operator manipulates a master or haptic device, and the generated position and/or force information from the master is sent to the slave robot through the communication channel. Then the slave robot manipulates the remote object or interacts with the environment and sends back the position and/or sensed contact force back through communication channel to the master for the operator's perception. Generally, bilateral teleoperation system can be considered as coupling together the subsystems: operator, master, communication channel, slave and environment. Position/velocity and force information are exchanged between each subsystem to realize bilateral teleoperation tasks. However, it is not straightforward to integrate force feedback into current RAS systems. The main factor that hinders this application is the limitations of the haptic/force sensor development which requests: (a) repeatability; (b) reliability; (c) speed of sensing; (d) response with static and dynamic; (d) size (limited to about 10mm in diameter for small port insertion); (e) sterilizability (using at least one commonly used sterilization method); (f) biocompatibility or with a protective sheath and (g) low cost, etc [20, 21]. The Da Vinci system provides surgeons with haptic feedback by utilizing sensory substitution to display the information through visual cues without using physical force sensors. It has been until very recently that the first commercial RAS system, the Senhance Surgical Robotic System by TransEnterix, with real force feedback thanks to its new unique force sensing system earned both FDA and CE marking approvals.

For safe and accurate bilateral teleoperation, *stability* and *transparency* are two essential features from control design point of view [7]. *Stability* means that the closed loop teleoperation system should maintain stability and be irrespective of the communication time delay, uncertainties of the operator and the environment dynamics. Some recent works addressing this issue can be found in [8, 9]. *Transparency*, also called telepresence, means that the teleoperation system should let the operator feel as if he/she is interacting with the environment directly. In bilateral teleoperation system, the operator and environment are connected by the master-slave-network (MSN) in which the communication channel serves an crucial role by exchanging necessary information (position/velocity and force). However, time delay is inevitable in communication channel because of data transmission, e.g. limited network bandwidth, transmitted data coding and decoding, internet/wireless communication, etc. [22–24].

Time delay in bilateral teleoperation represents one of the major challenges in the control design for both stability and transparency. It has been indicated that time delay makes the communication channel non-passive, and further causes the bilateral teleoperation system non-passive even unstable [28]. Without proper control strategy, small time delay (e.g. tens of milliseconds) can destabilize the bilateral teleoperation system [29], thus leading to high risk to the human operator and the environment. A large number of researchers have proposed methods to make a trade-off between stability and transparency as reported in literature [30–34]. The wave variable transformation (WVT) structure was first proposed in [29] to systematically handle the instability issue caused by constant time delay in bilateral teleoperation system. However, the poor tracking performance of WVT structure is observed which is due to the conservative condition of the wave variables construction. The degraded tracking performance limits the application of WVT structure, thus motivates many researchers to propose new structure to improve the tracking performance.

In [35] and [36], two modified wave variable structures have been proposed, and the performances have been enhanced by reducing the influence of the bias terms in traditional force and velocity/position tracking of WVT. But the tracking performances are not satisfactory since they still suffer from bias terms which involve master/slave velocity/force information and wave impedance b. In [37] and [38], different augmented wave variable structures are designed to improve the tracking performance of WVT by introducing augmented wave variable terms. Yet, the improvement is limited since for each single structure only one tracking performance (either force or velocity/position) can be improved but not both. In [39], a wave variable based structure is proposed to provide stable tracking performance, energy reservoir based regulators are designed to guarantee the passivity of the system. However, further analysis of the passivity and transparency of the proposed method is not provided which may not achieved stable and improved tracking performance when the energy reservoir based regulator is not properly defined. In our previous study [43], a novel wave based structure is designed to achieve enhanced tracking performance, in which a Kalman filter based predictor is utilized to predict the backward wave variable at the master side, thus single time delayed position tracking and even smaller force tracking performance can be obtained thanks to the predictor used in the structure. Still, comprehensive analysis of the role of the energy reservoir based regulator is not provided and only simulation studies were conducted. More complete literature survey can be found in [40–42] for further reading.

In this paper, a new wave variable compensation (WVC) bilateral teleoperation structure has been proposed for robotic-assisted surgery applications based on our previous works [26, 43]. The performance of the proposed approach has been verified through both simulation and experimental studies. The novelties of this work mainly lie in: (1) enhanced tracking performance and therefore

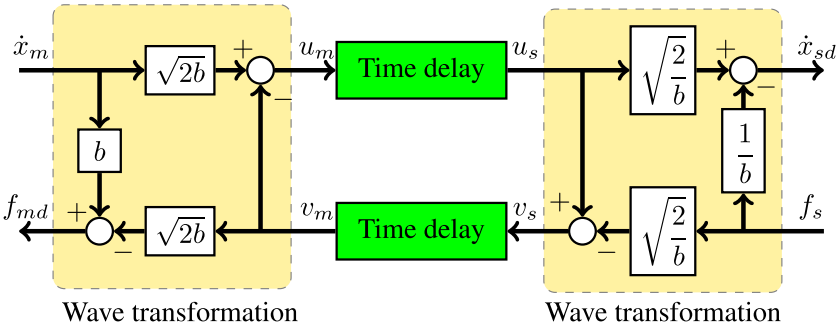

Fig. 1 Basic WVT structure

system transparency is achieved, and the improvements of velocity/position and force tracking are quantitatively analyzed; (2) energy reservoir based regulators are used to guarantee the passivity of the proposed structure, the role of energy reservoir based regulators is investigated in depth through both simulation and experimental studies for the first time in literature; (3) for certain operations such as microsurgery where scaled tracking is needed, a scaled WVC structure is developed with passivity and transparency conditions explicitly defined; (4) performance comparisons with several recent major modified wave variable structures are provided through simulation studies.

The rest of this paper is organized as: in Section 2, the fundamentals of WVT structure is introduced; in Section 3 the new wave variable compensation (WVC) structure is introduced; passivity and transparency analysis of the proposed scaled WVC approach is conducted in Section 4; in Section 5, simulation and experimental studies are performed to verify the performance of proposed WVC and scaled WVC approach. The last section of this paper summarizes the presented work and give some conclusions.

2 Fundamentals of Wave Variable Structure

From energy point of view, the WVT approach is proposed based on passivity theory in [29] to stabilize the communication channel with time delay, in which, the transmitted information between master and slave are wave variables which are constructed from the force and velocity information. Fig. 1 illustrates the WVT structure and Fig. 2 shows an equivalent structure of the WVT.

The forward and the backward wave variables u_m and v_s are constructed as in *wave transformation* block of Figs. 1 and 2:

$$u_m(t) = \frac{1}{\sqrt{2b}}(f_{md}(t) + b\dot{x}_m(t)) \tag{1}$$

$$v_s(t) = \frac{1}{\sqrt{2b}}(-f_s(t) + b\dot{x}_{sd}(t)) \tag{2}$$

where f_{md} and $\dot{x}_{sd}$ denote the reflected force from the slave to the master and the desired velocity of the slave respectively, f_s and $\dot{x}_m$ represent the interaction force of the slave with the environment and the master command velocity respectively. b is the wave impedance parameter without unit which allows the designer to make trade-off between mass and stiffness properties of the teleoperation system [44]. Accordingly, the wave variables u_s and v_m can also be obtained as:

$$u_s(t) = \frac{1}{\sqrt{2b}}(f_s(t) + b\dot{x}_{sd}(t)) \tag{3}$$

$$v_m(t) = \frac{1}{\sqrt{2b}}(-f_{md}(t) + b\dot{x}_m(t)) \tag{4}$$

Assume that the communication time delay T between the master and slave is constant, then the relationship of the wave variables can be described as:

$$u_s(t) = u_m(t - T) \tag{5}$$

$$v_m(t) = v_s(t - T) \tag{6}$$

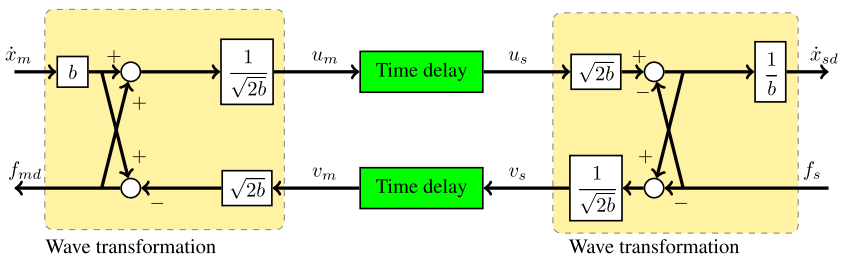

Fig. 2 Basic WVT structure (equivalent structure)

From Eqs. 1 – 4, the force and velocity information from both master and slave sides can be derived in the form of wave variables as:

$$f_{md}(t) = \frac{b}{\sqrt{2b}}(u_m(t) - v_m(t)) \tag{7}$$

$$\dot{x}_m(t) = \frac{1}{\sqrt{2b}}(u_m(t) + v_m(t)) \tag{8}$$

$$f_s(t) = \frac{b}{\sqrt{2b}}(u_s(t) - v_s(t)) \tag{9}$$

$$\dot{x}_{sd}(t) = \frac{1}{\sqrt{2b}}(u_s(t) + v_s(t)) \tag{10}$$

The passivity of the WVT is guaranteed by calculating the energy entered into the 2-port communication system using Eqs. 7–10 as [29]:

$$\begin{aligned} E(t) &= \int_0^t (f_{md}(\tau)\dot{x}_m(\tau) - f_s(\tau)\dot{x}_{sd}(\tau))d\tau \\ &= \tfrac{1}{2}\int_{t-T}^t u_m(\tau)u_m(\tau)d\tau + \tfrac{1}{2}\int_{t-T}^t v_s(\tau)v_s(\tau)d\tau \geq 0 \end{aligned} \tag{11}$$

From Eqs. 11, it can be seen that there is always positive energy flowing into the communication channel. Moreover, the positiveness of energy entered into the system is not affected by the time delay T, which indicates that the WVT structure can theoretically tolerate arbitrary time delay.

The tracking performance of the WVT can be obtained from Eqs. 5–10 as:

$$\dot{x}_{sd}(t) = \dot{x}_m(t-T) + \frac{1}{b}(f_{md}(t-T) - f_s(t)) \tag{12}$$

$$f_{md}(t) = f_s(t-T) + b(\dot{x}_m(t) - \dot{x}_{sd}(t-T)) \tag{13}$$

From Eqs. 12 and 13, it is clear that although WVT approach can guarantee passivity of the teleoperation system its velocity/position and force tracking performances are biased. Wave impedance b can be used to tune the tracking performance. However, the two desired tracking performances (force and velocity/position) are always conflicting as increasing one would degrade the other as seen in Eqs. 12 and 13.

3 Wave Variable Compensation (WVC) Structure

3.1 Structure Design

In view of the poor tracking performance of the WVT structure caused by the two bias terms from equation (12) and (13), in this section a new wave variable based structure is proposed suppress the bias terms by introducing two wave variable compensation terms such that tracking performances can be considerably improved.

In the WVT structure, the received wave variable v_m and u_s at both sides can be rewritten from Eqs. 7 and 10 as:

$$v_m(t) = u_m(t) - \sqrt{\frac{2}{b}} f_{md}(t) \tag{14}$$

$$u_s(t) = \sqrt{2b}\dot{x}_{sd}(t) - v_s(t) \tag{15}$$

In bilateral teleoperation without time delay, the ideal tracking performance prefers that the slave robot follows the motion of master exactly, meanwhile the feedback force on the master side follows faithfully the contact force on the slave side. When time delay exists in communication channel, the "optimal" delayed tracking performance can be naturally defined as:

$$\begin{cases} \dot{x}_{sd}(t) = \dot{x}_m(t-T) \\ f_{md}(t) = f_s(t-T) \end{cases} \tag{16}$$

meaning that the force and motion signals are tracked with only single time delay and the bias terms are removed.

In this optimal case, the relationship between constructed wave variables and force, motion as in Eqs. 14 and 15 can be re-written as:

$$v_m(t) = u_m(t) - \sqrt{\frac{2}{b}} f_s(t-T) \tag{17}$$

$$u_s(t) = \sqrt{2b}\dot{x}_m(t-T) - v_s(t) \tag{18}$$

According to Eqs. 8 and 9, $f_s(t-T)$ and $\dot{x}_m(t-T)$ can be represented in form of wave variables as below:

$$\dot{x}_m(t-T) = \frac{1}{\sqrt{2b}}(u_m(t-T) + v_m(t-T)) \tag{19}$$

$$f_s(t-T) = \frac{b}{\sqrt{2b}}(u_s(t-T) - v_s(t-T)) \tag{20}$$

Substituting Eqs. 19 and 20 into Eqs. 17 and 18, it has:

$$v_m(t) = v_s(t-T) + \underbrace{u_m(t) - u_s(t-T)}_{\Delta v} \tag{21}$$

$$u_s(t) = u_m(t-T) + \underbrace{v_m(t-T) - v_s(t)}_{\Delta u} \tag{22}$$

Comparing to the wave variable relationships in conventional WVT as in (5) and (6), it is seen from Eqs. 21 and 22 that if the "optimal" tracking goal is to be satisfied, the received wave variables at the slave side ($u_s(t)$) and the master side ($v_m(t)$) should contain two compensation terms (Δu and Δv) compared with original WVT terms (where $u_s(t) = u_m(t-T)$ and $v_m(t) = v_s(t-T)$).

Following this design philosophy, a new structure with two wave variable compensation terms can be proposed as illustrated in Fig. 3, where the compensation term $\Delta u(t) = \Delta u_1(t-T) - \Delta u_2(t)$ and $\Delta v(t) = -\Delta v_1(t-T) + \Delta v_2(t)$. Theoretically, this structure could achieve an "optimal" tracking performance. However, it should be noticed that injecting two wave variable compensation terms may cause the structure non-passive. Fig. 4 shows the WVC structure

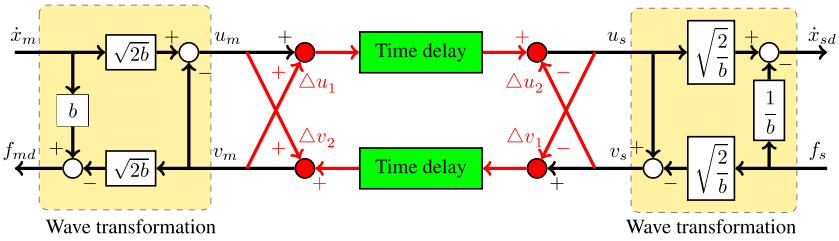

Fig. 3 Wave variable compensation approach

by incorporating the WVC terms into the communication channel.

Remark 1 Different from the method in [39], in this proposed method no wave impedance matching is needed and consequently the construction of wave variables (u_m, v_m, u_s, v_s) remains simple and unchanged such that existing predication methods, e.g. [45], could be easily applied to further improve the system performance.

3.2 Passivity Using Energy Reservoir Based Regulators

Energy reservoir based regulator was firstly designed in [46] to modulate the injected energy in the wave variable structure, and later has been explored in [45, 47]. In this work, as compensations are made by adding Δu (between $u_s(t)$ and $u_m(t-T)$) and Δv (between $v_m(t)$ and $v_s(t-T)$), the resulting injected energy eventually flows into the whole system and may potentially destroy the passivity. Since the power can be represented as the product of wave variables [29], two energy reservoirs can be constructed in this work as:

$$E'_s(t) = \int_0^t \left(u_m^2(t-T) - v_s^2(t)\right) dt \tag{23}$$

$$E'_m(t) = \int_0^t \left(v_s^2(t-T) - u_m^2(t)\right) dt \tag{24}$$

The two constructed energy reservoirs track the amount of the energy introduced by the two wave variable compensation terms into the slave side (including the slave and the WVT with $u_m(t-T)$ as the input and the $v_s(t)$ as the output) as in (23) and the master side (including the master and the WVT with $v_s(t-T)$ as the input and the $u_m(t)$ as the output) as in (24) respectively.

Assuming that energy reservoirs are not empty during the teleoperation task, the compensation terms can be modified as follows in order to ensure system passivity:

$$\Delta u' = \alpha \left[1 - e^{-\beta E'_s(t)}\right] (v_m(t-T) - v_s(t)) \tag{25}$$

$$\Delta v' = \alpha \left[1 - e^{-\beta E'_m(t)}\right] (u_m(t) - u_s(t-T)) \tag{26}$$

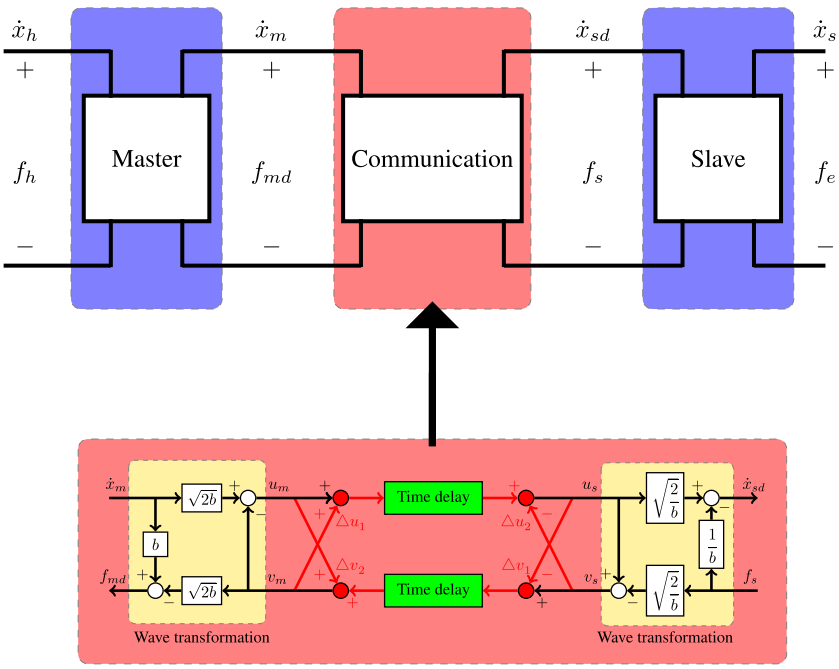

Fig. 4 Cascaded bilateral teleoperation with WVC structure

The α and β are parameters to regulate the compensation terms, and $E'_m(t)$ and $E'_s(t)$ are two defined energy reservoirs located at both master and slave side. Because of the new wave variable compensation terms, extra energy will be injected into the system. Taking the master side for example, during the teleoperation task, the master is usually assumed to perform passively ($(E_m(t)) \geq 0$). With continuous compensation, the energy reservoir $E'_m(t)$ may decrease due to the extra energy caused by the compensation term Δu. When the value of the energy reservoir $E'_m(t)$ drops to 0, the regulation terms $\alpha\left[1-e^{-\beta E'_m(t)}\right]$ becomes 0, hence the compensation term $\Delta v = 0$, and the wave variable compensation term is switched off. In this case, the WVC structure becomes the original WVT structure and the passivity of the system is always guaranteed (Fig. 5).

Discussions

1. The regulation terms $\alpha\left[1-e^{-\beta E'_m(t)}\right]$ and $\alpha\left[1-e^{-\beta E'_s(t)}\right]$ determine how much of compensation will be injected into the teleoperation system. In ideal case ($E'_m \to \infty$, $E'_s \to \infty$), the regulation terms equal to 1 ($\alpha\left[1-e^{-\beta E'_m(t)}\right]=1$ and $\alpha\left[1-e^{-\beta E'_s(t)}\right]=1$). However, with the compensated terms, extra energy may be introduced into the system which drains the energy reservoir ($E'_m(t)=0$ or $E'_s(t)=0$) until the compensation is choked off , especially for big time delay bilateral teleoperation system since bigger time delay normally cause more energy induced [29].
2. A proper selection of the parameters α, β and the initial value of the energy reservoirs ($E'_m(0)$ and $E'_s(0)$) is important for the performance of the WVC structure. Some guidelines are given as follows:

   (1) α is a positive parameter to determine the speed of regulation, and $0 < \alpha \leq 1$. Normally, α is chosen to 1 such that the compensation terms are not distorted in ideal case.

   (2) When $\alpha = 1$ is used, $1-e^{-\beta E'_m(t)}$ and $1-e^{-\beta E'_s(t)}$ play important roles to tune the WVC performance. β and the initial energy reservoir values are all positive such that $0 \leq 1-e^{-\beta E'_m(t)} \leq 1$ and $0 \leq 1-e^{-\beta E'_s(t)} \leq 1$. Without loss of generality, β could be assumed as $\beta = 1$ to facilitate analyzing the effect of the initial values of energy reservoirs on the compensation regulation:

   – The initial values for energy reservoir $E'_s(0)$ and $E'_m(0)$ should be sufficiently large, otherwise the compensation terms will be easily choked off even at the beginning of the teleoperation task since the regulation margin is too small.

   (3) β and the initial energy reservoir values are used in combination for the regulation of the wave variable compensation terms. The choice/tuning of the initial values of the energy reservoirs and β is usually empirical because they are system-dependent and also depends on the teleoperation tasks to be carried out which are difficult (sometime impossible) to predict in advance.

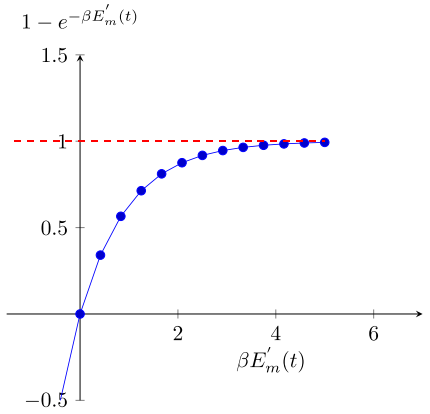

Fig. 5 Effect of control parameters (energy reservoir $E'_m(t)$ and β) on the regulation of compensation terms

Remark 2 This is the first time that the analysis of energy reservoir based regulator is performed within wave based teleoperation structures. In the previous studies on wave based bilateral teleoperation method, the energy reservoir based regulator are used with the assumption that the master, slave, operator and environment are all passive, which is not possible in practice. The analysis of the energy reservoir based regulator now can provide the guideline for using this technique in future bilateral teleoperation system design. The effect of the parameters in energy reservoir based regulator is also provided in the experimental studies.

4 Scaled Bilateral Teleoperation with WVC

For many bilateral teleoperation applications, to scale up or down the force and position information can bring benefits to both the operator and the teleoperation tasks. In robotic-assisted microsurgery, scaling down robot's motion and scaling up force feedback to the operator are necessary. With the scaled force and motion, the robot can move slowly and more precisely to avoid unexpected damage to the delicate tissues during the operation and even light interaction with the tissue can be felt by the operator to

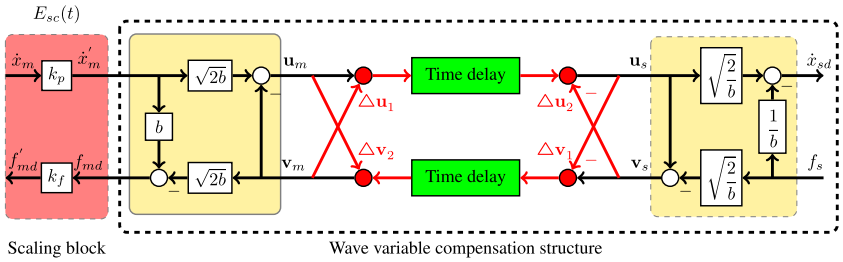

Fig. 6 Scaled WVC approach

facilitate manipulation tasks with high safety requirement. In order to achieve scaled performance, two scaling factors k_p and k_f are used to scale the position/velocity and force information between the master and slave sides. The scaling factors are defined by the human operator with consideration of the specific teleoperation task.

Based on the WVC structure developed in the previous section, a new scaled WVC structure can be designed. In the new scaled WVC structure, two scaling factors k_p and k_f are located between the master and the communication channel, as shown in Fig. 6. The master velocity $\dot{x}_m$ is scaled by k_p such that the scaled velocity $\dot{x}'_m$ is transmitted to the WVC system. Similarly, the feedback force f_{md} is scaled by k_f and the scaled force f'_{md} is reflected to the master. In practice, the location of the scaling factors are set on the master console in order to facilitate the surgeon's tuning.

The scaling block shown in Fig. 6 can be considered as a 2-port system $E_{sc}(t)$, through which the scaled signals can be obtained as:

$$\dot{x}'_m(t) = k_p \dot{x}_m(t) \tag{27}$$

$$f'_{md}(t) = k_f f_{md}(t) \tag{28}$$

such that the tracking performance as in (16) are re-written as

$$\begin{cases} \dot{x}_{sd} = k_p \dot{x}_m(t-T) \\ f'_{md} = k_f f_s(t-T) \end{cases} \tag{29}$$

4.1 Stability Analysis

To analyze the proposed scaled WVC structure, the passivity of the scaling block is examined. The energy flowed into the scaling block E_{sc} can be calculated as:

$$\begin{aligned} E_{sc} &= \int_0^T P d\tau = \int_0^T P_{in} d\tau - \int_0^T P_{out} d_\tau \\ &= \int_0^T \dot{x}_m(t) f'_{md}(t) d\tau - \int_0^T \dot{x}'_m(t) f_{md}(t) d\tau \\ &= \int_0^t (\dot{x}_m(t) f'_{md}(t) - \dot{x}'_m(t) f_{md}(t)) d\tau \\ &= \int_0^t (\dot{x}_m(t) f'_{md}(t) - k_p \dot{x}_m(t) \frac{1}{k_f} f'_{md}(t)) d\tau \\ &= \int_0^t (1 - \frac{k_p}{k_f})(\dot{x}_m(t) f'_{md}(t)) d\tau \\ &= (1 - \frac{k_p}{k_f}) \int_0^t (\dot{x}_m(t) f'_{md}(t)) d\tau \end{aligned} \tag{30}$$

In bilateral teleoperation system, the scaled WVC block can be cascaded with the *operator*, *master*, *slave* and *environment* as shown in Fig. 7, where the cascaded operator and master are considered as a 1-port system as enclosed by the dashed line. f'_{md} and $\dot{x}_m$ represent the input and output of the 1-port system. Usually the operator and the master are assumed to be passive so that it has:

$$E = \int_0^t (\dot{x}_m(t) f'_{md}(t)) d\tau \geq 0 \tag{31}$$

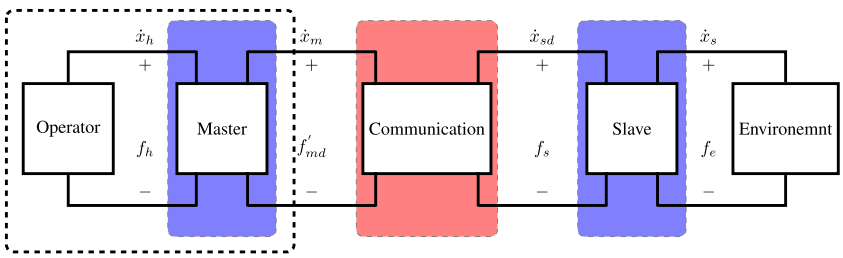

Fig. 7 Scaled WVC structure in bilateral teleoperation system

Therefore, the passivity condition to guarantee the passivity of the scaling block can be obtained from Eqs. 30 and 31 as:

$$1 - \frac{k_p}{k_f} \geq 0 \tag{32}$$

such that $E_{sc} = (1 - \frac{k_p}{k_f}) \int_0^t (\dot{x}_m(t) f'_{md}(t)) d\tau \geq 0$.

The passivity condition (32) of the scaling blocks can be rewritten as:

$$k_f \geq k_p \tag{33}$$

The condition (33) implies that the scaled WVC will keep passive if the force scale is greater than or equal to the position/velocity scale. In surgical application, especially microsurgeries, this condition is intrinsic and thus can be easily satisfied since the surgeon usually expect the robot to move slowly ($K_p < 1$) and the force to be augmented from safety consideration ($K_f > 1$).

4.2 Transparency Analysis

To analyze the transparency of the proposed scaled WVC structure, it is necessary to start with the transparency analysis of bilateral teleoperation without time delay as presented below.

4.2.1 Transparency of Scaled Bilateral Teleoperation Without Delay

Figure 8 provides the schematic of scaled bilateral teleoperation system, in which the human operator and environment are represented with the impedance Z_h ($Z_h = F_h/\dot{X}_h$) and Z_e ($Z_e = F_e/\dot{X}_s$). The operator manipulates the master and sends the velocity $\dot{x}_m$ modified by the position/velocity scaling factor k_p. The scaled velocity information $\dot{x}'_m$ is transmitted through the communication and drives the slave robot to contact the environment at the desired velocity $\dot{x}_{sd}$. Similarly, the feedback force f_{md} is scaled by the force scaling factor k_f, and the scaled force f'_{md} is felt by the human operator. Note that the scaling factors k_p and k_f can also be placed between the communication channel and the slave.

Assuming that the operator is holding the master device to move and can felt the immediate force feedback f'_{md}, the impedance felt by the operator Z_{felt} can be derived as:

$$Z_{felt} = \frac{F'_{md}}{\dot{X}_m} \tag{34}$$

and it should be noted that $Z_{felt} \neq Z_h$.

In ideal case (no time delay and no losses in master and slave system due to friction and compliance), it has:

$$\dot{x}_s = \dot{x}_{sd} = \dot{x}'_m = k_p \dot{x}_m \tag{35}$$

$$f'_{md} = k_f f_{md} = k_f f_s = k_f f_e \tag{36}$$

then the felt impedance Z_{felt} can be rewritten as:

$$Z_{felt} = \frac{F'_{md}}{\dot{X}_m} = \frac{k_f F_e}{\frac{1}{k_p}\dot{X}_s} = k_p k_f \frac{F_e}{\dot{X}_s} = k_p k_f Z_e \tag{37}$$

In a transparent bilateral teleoperation system, the impedance felt by the operator should be as close as the environment impedance [44]. To provide perfect transparency to the operator in the scaled bilateral teleoperation, the scaling factors should satisfy the following condition:

$$k_p k_f = 1 \tag{38}$$

4.2.2 Transparency of Scaled WVC Structure

In the scaled bilateral teleoperation system with presence of time delay, the felt impedance by the operator is still calculated as:

$$Z_{felt} = \frac{F_{md}\prime}{\dot{X}_m} \tag{39}$$

From Eq. 29, it has

$$\begin{cases} \dot{x}_m = \frac{1}{k_p}\dot{x}_s(t+T) \\ f'_{md} = k_f f_s(t-T) \end{cases} \tag{40}$$

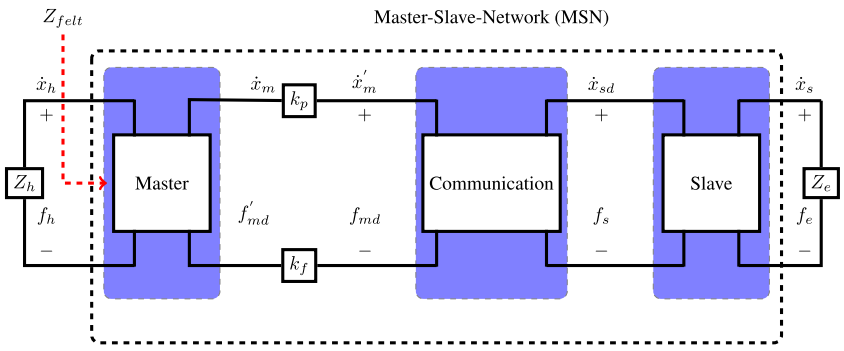

Fig. 8 Scaled bilateral teleoperation system

such that Z_{felt} can be further written as:

$$Z_{felt} = \frac{F_{md}{}'}{\dot{X}_m} = \frac{\mathcal{F}[f'_{md}](\omega)}{\mathcal{F}[\dot{x}_m](\omega)} = \frac{k_f \mathcal{F}[f_s(t-T)](\omega)}{\frac{1}{k_p}\mathcal{F}[\dot{x}_s(t+T)](\omega)} \quad (41)$$
$$= k_f k_p \frac{e^{-iT\omega}\mathcal{F}[f_s(t)](\omega)}{e^{iT\omega}\mathcal{F}[\dot{x}_s(t)](\omega)} = k_p k_f e^{-2iT\omega}\frac{F_e}{\dot{X}_s}$$
$$= k_p k_f e^{-2iT\omega} Z_e = k_p k_f \cdot Z_e \underline{/-2T\omega}.$$

It is seen that the reflected/felt impedance Z_{felt} has amplitude change by $k_p k_v$ and phase shift by $-2T\omega$ from the real environment impedance Z_e.

To maximize the impedance match (transparency), it needs to minimize both the amplitude and phase changes. If $k_p k_v = 1$, then $Z_{felt} = Z_e \underline{/-2T\omega}$ and it guarantees that the felt impedance has the same amplitude as the real impedance Z_e. With $k_p k_v = 1$ satisfied, the phase change $\underline{/-2T\omega}$ is better explained in time domain and means that the operator feels the true remote impedance with a delay time of $2T$. This delay is system-specific and is not affected by the interaction frequencies involved.

Therefore, the maximized transparency of our scaled bilateral teleoperation system can be obtained if the pre-defined scale parameters satisfy

$$k_p k_v = 1. \quad (42)$$

Based on the analysis above, the scaled WVC structure facilitates the robotic-assisted microsurgery if both passivity and transparency conditions Eqs. 33 and 42 are satisfied.

Remark 3 For traditional WVT structure, it is difficult to quantitatively evaluate the system transparency and furthermore to derive the maximal transparency condition. In this work, the stability and transparency of the proposed WVC structure are analyzed in details which is not well addressed in many works including [39].

5 Simulation and Experimental Studies

5.1 Time Delay Investigation in OR set up

Before starting the simulation and experimental studies, it is necessary to identify the time delay that exist in teleoperation of robotic-assisted surgery (RAS). In this work, the application of miniaturized surgical robotic system is considered [25], where time delay is often caused by replacing the physical communication cables with wireless data transmission and hence inevitably leads to considerable communication delay. In fact, driven by the needs for enhanced cosmetic benefits and reduced morbidity risks associated with multiple incisions, RAS has evolved from robotic minimally invasive surgery (RMIS) to single-port laparoscopy (SPL) and then to natural orifice transluminal endoscopic surgery (NOTES). Robotic intervention and diagnosis techniques with less or even no physical cables/wires are foreseen as future trends of RAS.

In our previous study of miniaturized surgical robot system [26], the Zigbee protocal has been chosen among Wi-Fi and Bluetooth wireless communication protocals for data transmission between master console and the miniaturized slave robot due to its advantages in terms of size, power consumption, latency, robust performance and tolerance to environment interference, etc. Considering specialized OR(operation room) for transplants may require 750-800 sq ft (70-75 m2) [27], and all devices located inside OR may be potential interference sources, experiments have been carried out under different operating room (OR) set-ups:

Group 1: Two Zigbee communication boards were located close (with distance of 10cm);
Group 2: Two Zigbee communication boards were located close (with distance of 10cm) but with mobile phone between two boards which was in call;
Group 3: Two Zigbee communication boards were located with distance of 8 meters;
Group 4: Two Zigbee communication boards were located with distance of 6 meters and with obstacle between two boards.

In the communication experiments, UDP packets containing 32 bytes data were transferred between the two boards, and RTT (Round Trip Time) was recorded. The RTT experimental setup is shown in Fig. 9a, and it can be observed in Fig. 9b that the RTT caused by Zigbee communication is almost constant to 135ms with less than 1 ms variation. This experimental investigation justifies the constant time delay hypothesis for at least certain robotic surgery applications and also provides the basis for the following simulation and experimental studies.

5.2 Simulation Studies and Analysis

In order to validate the efficiency of the WVC and scaled WVC approach, simulation studies have been carried out based on a system as shown in Fig. 10. Here, without loss of generality, only one DoF is considered since both master and slave dynamics could be linearized through inverse inverse dynamics calculation even if they might be nonlinear. A mass-damper system is used to model both master device and slave robot with the the dynamics as follows:

$$M_m \dot{x}_m + B_m x_m = f_h - f_{md} \quad (43)$$
$$M_s \dot{x}_s + B_s x_s = f'_s - f_s \quad (44)$$

where M_m and M_s describe the inertia's of the master and slave, and B_m and B_s are the damping coefficients.

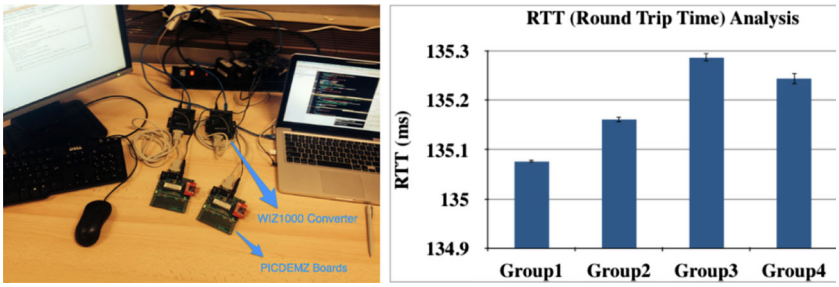

Fig. 9 Experimental set-up of Zigbee wireless communication

(a) RTT Experimental Setup (b) RTT delay in different situatuions

f_h denotes the force of the operator exerted during the teleoperation which is designed to follow a sinusoidal form as $f_h(t) = \sin(\omega t)$ in this study; f_{md} is the feedback force at the master side; f_s' represents the force of the slave robot generated from controller; f_s is the contact force between the slave robot and environment. In order to better model the environment, the Kelvin-Boltzmann (K-B) model [48] is used to mimic the soft tissue considering the accuracy of robot-tissue interaction, as shown in Fig. 11. Detailed parameters used for the simulation studies are provided in Table 1. The single-trip time delay T used in simulation studies is set to $200ms$.

In this simulation study, the performances of teleoperation systems with direct force feedback and WVT structures are compared with those of the new WVC and scaled WVC structure that we propose in this work to illustrate the performance improvements. Also, in order to justify the advantage of the proposed structures, simulation studies based on several representative wave based methods in literature are carried out for comparison purpose.

5.2.1 Direct Force Feedback Structure

The first simulation is conducted with the *direct force feedback* bilateral teleoperation system (in this structure, force and velocity signals are exchanged directly through the communication channel), the illustration of the system is shown in the Fig. 10. In this simulation study, the delayed communication is used to connect the master and slave system. The master velocity $\dot{x}_m$ and desired slave velocity $\dot{x}_{sd}$, the contact force at slave side f_s as well as feedback force at the master side f_{md} are recorded. Meanwhile, the energy entered into the communication channel $(\int_0^t (f_{md}(t)\dot{x}_m(t) - f_s(t)\dot{x}_{sd}(t))d\tau)$ is also calculated. The simulation result in Fig. 12 shows that the bilateral teleoperation system becomes unstable when time delay is $200ms$, and the energy entered into the communication channel is negative, which is consistent with the theoretical analysis that delayed communication channel is non-passive and makes the overall teleoperation system unstable.

5.2.2 WVT Structure

This simulation is conducted with the same configuration in Fig. 10, but with the *WVT structure* employed in the communication channel. Different wave impedance values of b lead to different tracking performances but this won't change the main conclusion to be obtained. Given the specific simulation setup, the value of b in this study is set to 40 through trials to better illustrate the tracking performance of WTV. $\dot{x}_m$, $\dot{x}_{sd}$, f_s and f_{md} are recorded in the same way as in previous simulation study, and the energy entered into the communication channel $(\int_0^t (f_{md}(t)\dot{x}_m(t) - f_s(t)\dot{x}_{sd}(t))d\tau)$ is also calculated.

From Fig. 13, it is noticed that stable tracking performance can be obtained, although significant tracking errors exist which is consistent with Eqs. 12 and 13 and caused by the bias terms. The passivity of the WVT

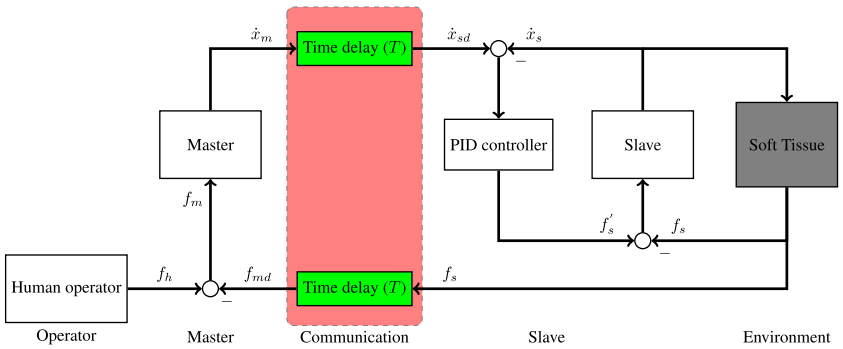

Fig. 10 Simulation configuration of one DoF teleoperation system

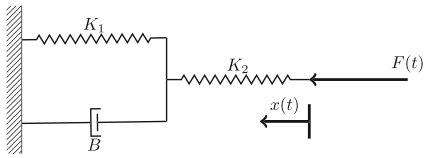

$$F(t) = \alpha_1 \dot{x}(t) + \beta_1 x(t) - \gamma_1 \dot{F}(t)$$

$$\alpha_1 = B\frac{K_2}{K_1+K_2}, \beta_1 = \frac{K_1 K_2}{K_1+K_2}, \gamma_1 = \frac{B}{K_1+K_2}$$

Fig. 11 Soft tissue model (Viscoelastic K-B model) [49]

structure is always guaranteed, as indicated by the energy stored in the communication channel.

5.2.3 WVC Structure

To analyze the performance of the WVC structure, the velocity and force information on both master and slave sides are recorded. Since the energy reservoir based regulators are used in the WVC structure, $E'_m(t)$ and $E'_s(t)$ as defined in (23) and (24) are also provided to analyze the passivity of the system. Meanwhile, $E_c(t)$ are defined as the energy stored in the communication channel $E_c(t) = \int_0^t (u_m(t)v_m(t) - u_s(t)v_s(t))d\tau$.

The simulation results are provided in Fig. 14. It is observed that the tracking performance of WVC structure in terms of force and velocity are greatly enhanced compared with the WVT structure under the same simulation configurations. The slave robot moves with around single time delayed master motion, and the feedback force at the master side are close to the contact force at the slave side. As seen in Fig. 14, $E'_s(t)$ and $E_c(t)$ in slightly increasing during the teleoperation, while $E'_m(t)$ decreases with around 0.06J during 40 seconds. The passivity of the system is always guaranteed since that all these energy changes ($E'_s(t)$, $E'_m(t)$ and $E_c(t)$) during the teleoperation keep positive.

To better illustrate the tracking performances and verify if the results meet the theoretical expectation as in Eq. 16, the master velocity command and the slave force feedback signals have been shifted by one single trip time (200ms) and the compared with the slave velocity and master perceived force signals as shown in Fig. 15, where the shifted tracking errors are also plotted. It is seen that the master and slave velocity and force signals overlap closely and the tracking errors are very small after the single trip time shift. This indicates that "optimal" tracking performance in face of constant time delay can be obtained with the proposed WVC structure and is consistent with the theoretical analysis of WVC structure as presented in Section 3.

Table 1 Parameters for simulation studies [49, 50]

Master	Mm (kg)	0.70
	Bm (Ns/m)	29.4
	Ms (kg)	1.0
Slave	Bs (Ns/m)	0.1
Environment	α_1 (Ns/m)	30.76
	β_1 (N/m)	100.43
	γ_1 (s)	0.06

5.2.4 Comparisons with Other Wave Based Methods

In order to evaluate the performance of proposed WVC structure with respect to the state-of-the-art, we carried out comparative simulation studies with several existing wave based approaches in literature as introduced in [35–37] and [38].

In [35], a modified wave based controller was proposed to improve the force tracking and position tracking compared with WVT structure. An additional wave impedance α is implemented in the controller, thus changes the wave transformation of the traditional WVT structure. Passivity of the proposed approach can be retained if b and α are properly selected. In the simulation study of [35], b=α= 40 are chosen and its tracking performance can be seen in Fig. 16. It is observed that force tracking performance is improved but the slave velocity tracking still has significant overshoot. Both force and velocity cannot achieve single trip time (200ms) delayed tracking performance.

In order to reduce wave reflection when operating in unknown environment, [36] proposed a new wave based teleoperator, which changed the way of wave transformation from traditional WVT structure. The velocity tracking of this approach can be improved in cases of time invariant or slowly time varying contact force on the slave side. A simulation study is carried out for this wave based teleoperator. In order to guarantee the passivity of this method, a big wave impedance b is selected as 600. As shown in Fig. 17, the velocity tracking is improved, as the slave robot follows quite well the velocity of the master, however the feedback force is degraded.

In [37] and [38], two different augmented wave based teleoperation structures were proposed, aiming at improving the force tracking and velocity tracking performance respectively. Additional wave variable terms were utilized in the augmented wave based method. Simulation studies are conducted to evaluate the performances of the two augmented wave based teleoperation structures. The tracking performance are presented in Figs. 18 and 19, and it is noticed that only velocity or force tracking can be improved to achieve around single trip time delayed tracking performance but not both at the same time.

Remark 4 Through comparative simulation studies with existing wave based teleoperation approaches, it is clearly

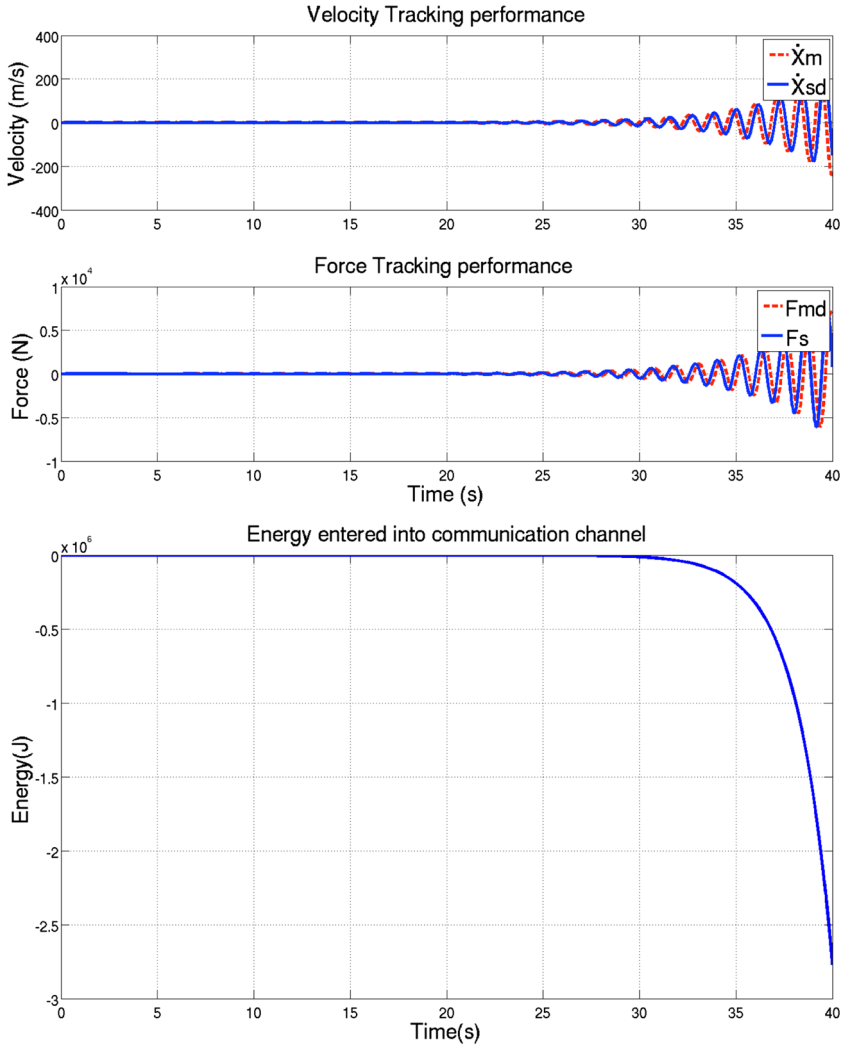

Fig. 12 Simulation results of ***direct force feedback*** bilateral teleoperation ***(200ms)***

shown that previous methods can only provide compromised tracking performance. In contrast, for the WVC approach proposed in this paper, with proper selection of control parameters, superior velocity and force tracking can be obtained at the same time. A comprehensive comparison of the wave based methods studied in this section is provided in Table 2.

5.2.5 Scaled WVC Structure

Similar setup as in 5.2.3 for WVC structure is used for the simulation study of scaled WVC structure. Following the passivity condition in Eq. 33 and transparency condition in Eq. 42 ($k_f \geq k_p$ and $k_f k_p = 1$), two simulation studies are performed with scaling factors pre-defined as:

1. $k_f = 2$ ***and*** $k_p = 0.5$.
2. $k_f = 20$ ***and*** $k_p = 0.05$.

Figures 20 and 21 show the simulation results of the two studies with different scales. From the simulation results, it is first noticed that stable force and position tracking performances can be achieved. To present the scaled tracking performance more clearly, $\frac{\dot{x}_{sd}(t)}{k_p}$ and $\frac{f'_{md}(t)}{k_f}$ are also calculated and illustrated, as shown in the simulation results where it's seen that the scaled back performances are very close to $\dot{x}_m$ and f_s with slight time delay (roughly one single trip time) which supports the theoretical analysis of the scaled WVC structure in terms of passivity and transparency derived in Section 4.

5.3 Experimental Studies and Analysis

In order to further validate the developed WVC and scaled WVC structures in practice, experimental evaluations were carried out using two Omega 7 devices (*Force Dimension, Switzerland*): one as a master and the other as a slave as shown in Fig. 22. An ATI Nano 17 F/T force sensor (*ATI Industrial Automation, United States*) is attached to the slave tip to measure the contact force during experiments. The two Omega 7 devices are physically connected by

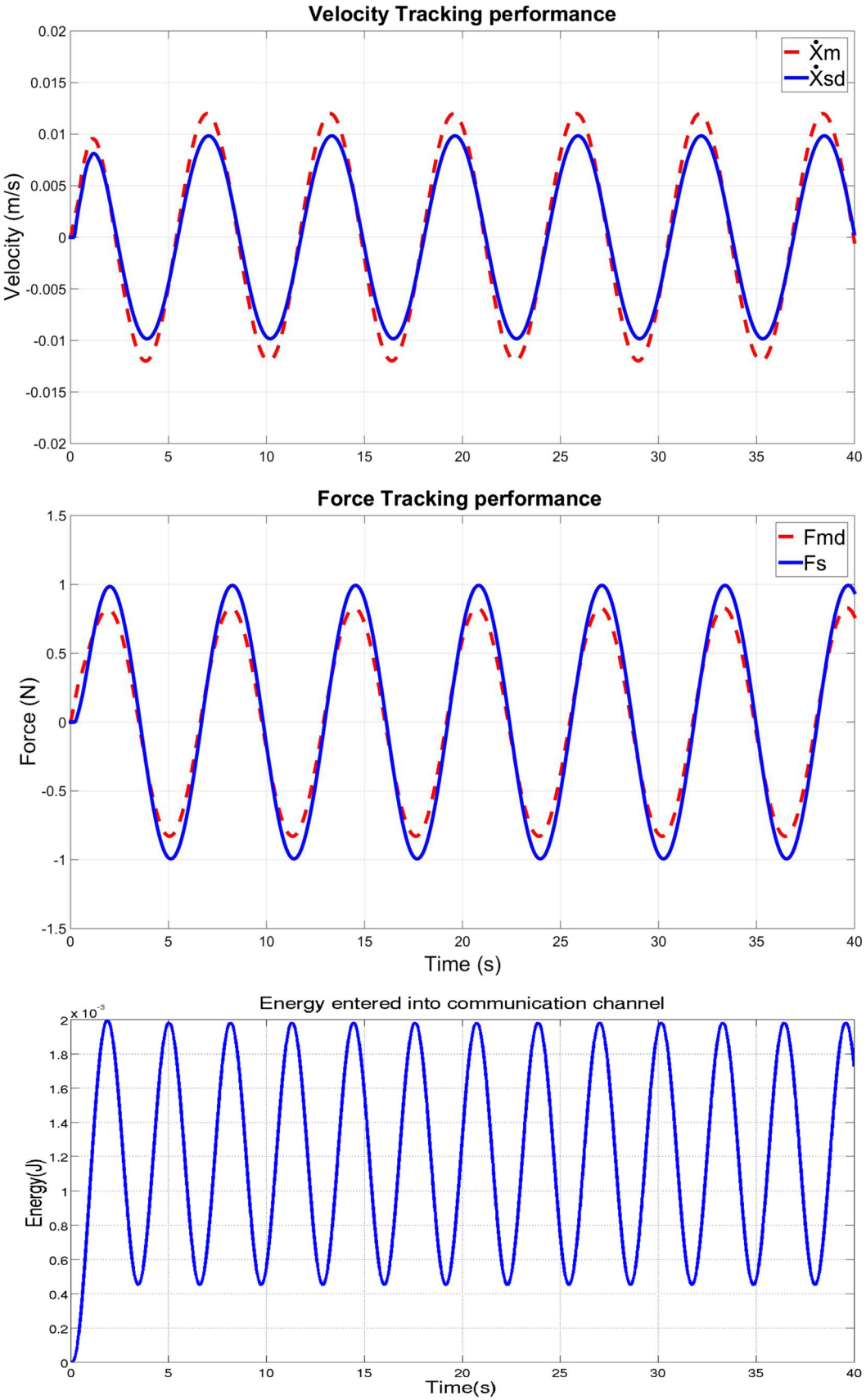

Fig. 13 Simulation results of ***WVT*** based bilateral teleoperation ***(200ms)***

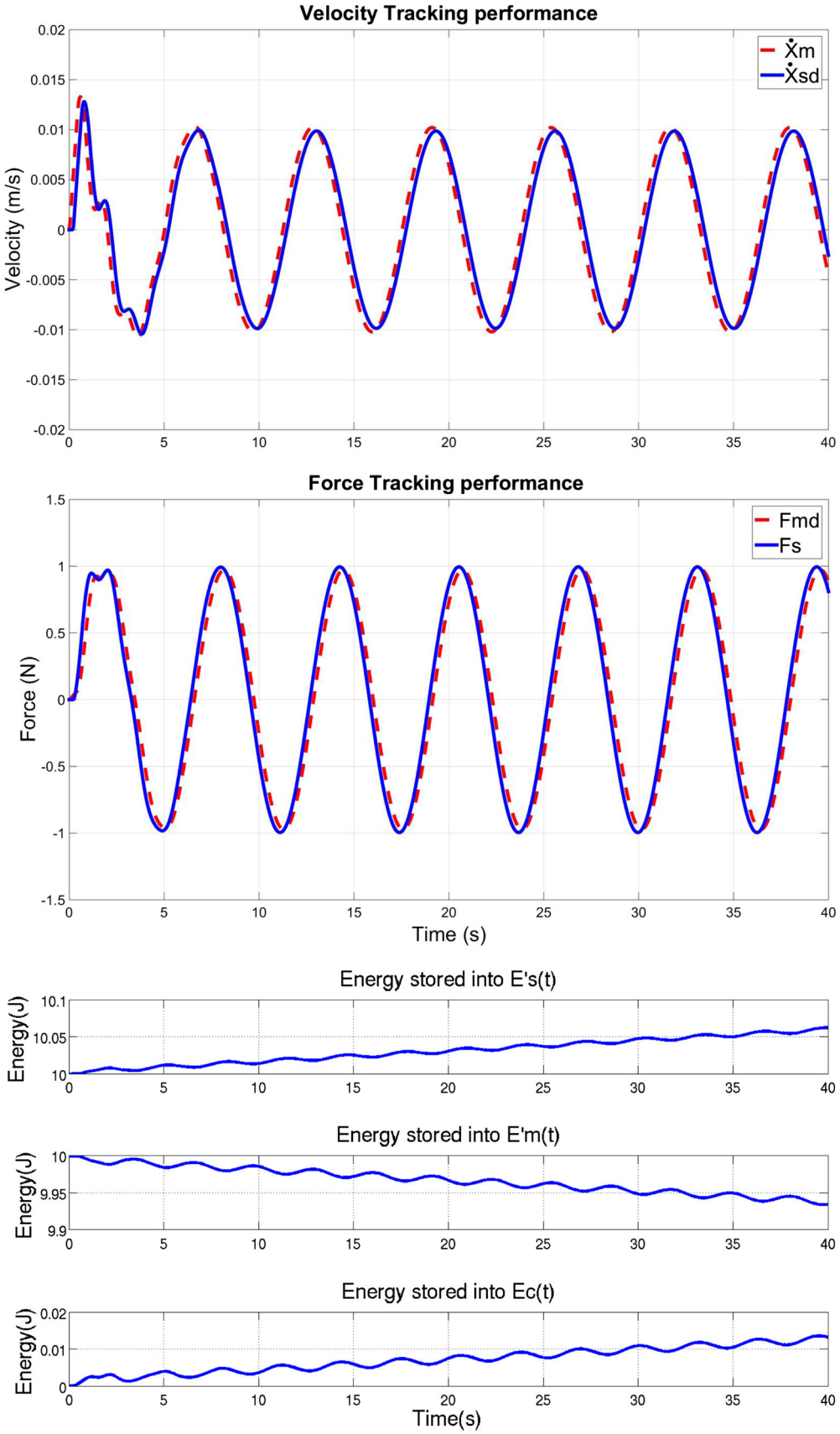

Fig. 14 Simulation results of ***WVC*** based bilateral teleoperation ***(200ms)*** and ***(*** $\alpha = 1$, $\beta = 0.2$ ***and*** $E'_m(0)$, $E'_s(0) = 10J$***)***

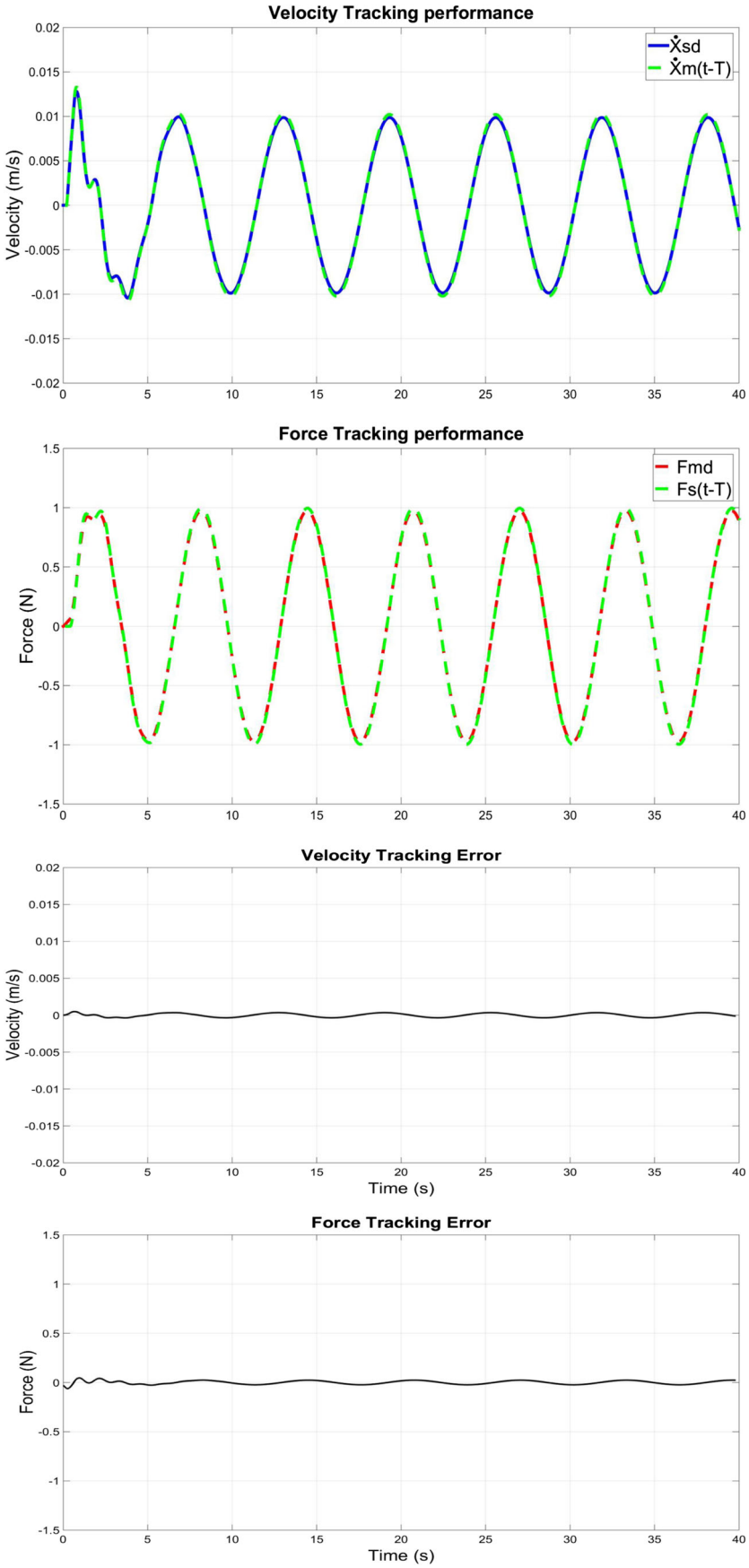

Fig. 15 Shifted velocity and force tracking performance of WVC based bilateral teleoperation

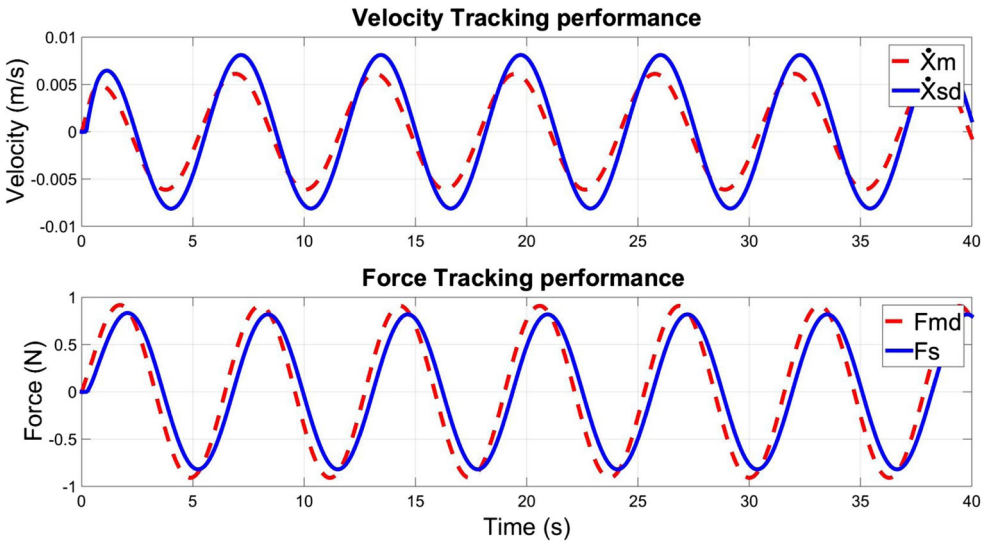

Fig. 16 Simulation results of [35] based bilateral teleoperation ***(200ms)*** with b***=40,*** $\alpha = 40$

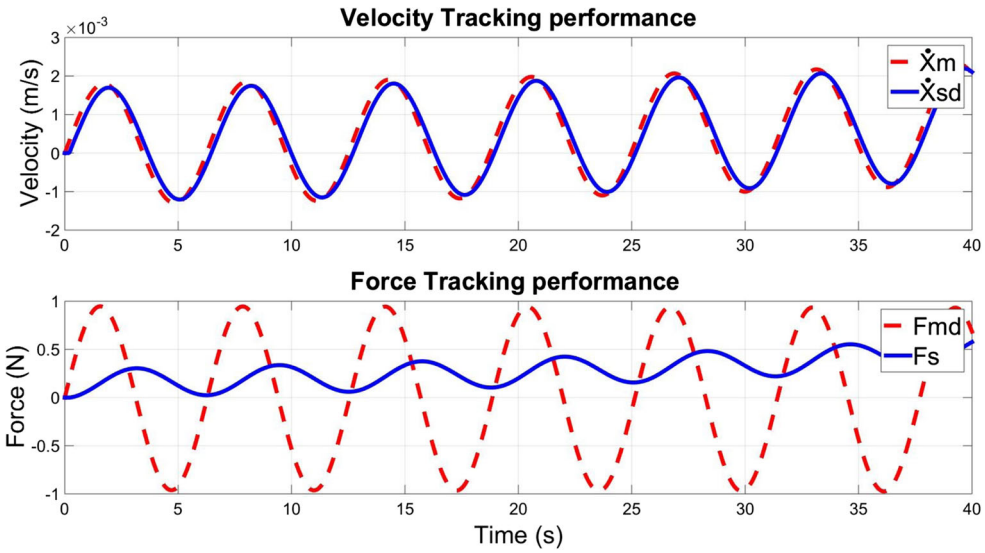

Fig. 17 Simulation results of [36] based bilateral teleoperation ***(200ms)*** with b***=600***

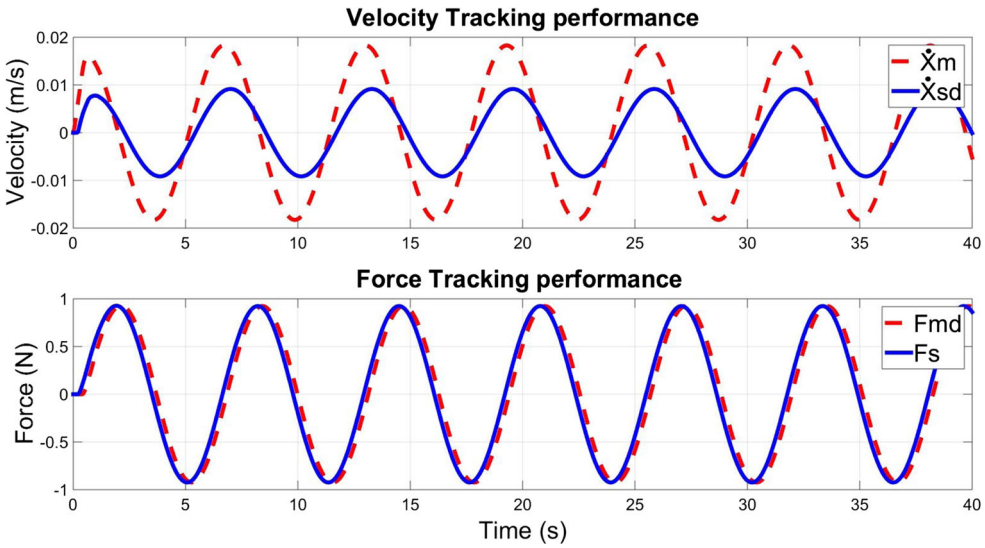

Fig. 18 Simulation results of [37] based bilateral teleoperation ***(200ms)*** with b***=40***

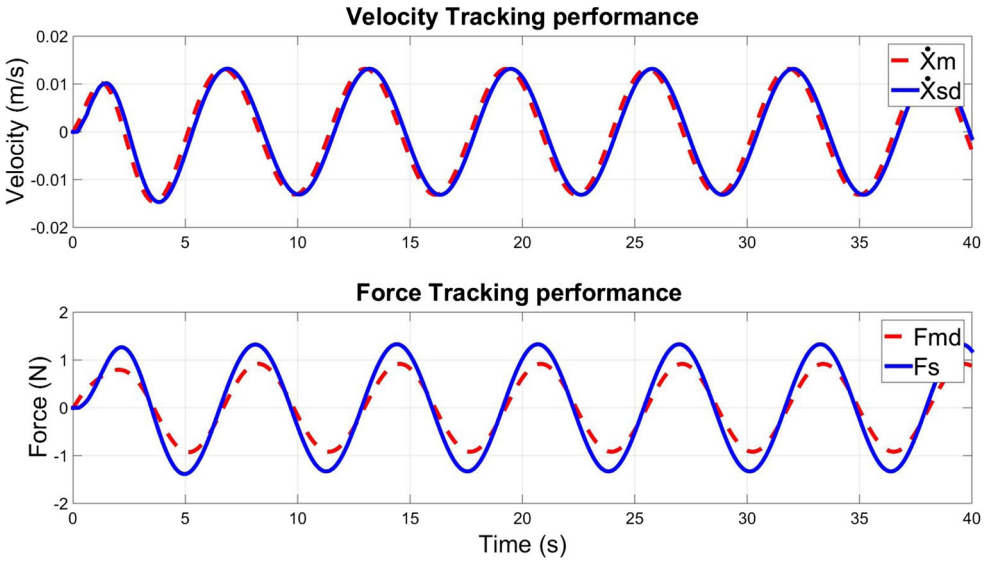

Fig. 19 Simulation results of [38] based bilateral teleoperation ***(200ms)*** with ***b=40***

Ethernet but with time delay intendedly set to 200ms to quantitatively evaluate the tracking performance. For the contact experiment, a two-layer synthetic phantom is used to mimic the human tissue [57, 58], which is made by extra soft PVC (80% soft PVC + 20% softener) and mediumdensity PVC (70% soft + 30% hard PVC). The master is running under Mac OS and the slave robot is running under Linux Ubuntu 12.04. The working frequency of the system is 1kHz. Direct force feedback experiment is not carried out due to safety consideration since from the simulation studies it is already shown that even with 200ms time delay in communication channel the system becomes unstable easily. In the experimental studies, only WVT, WVC and scaled WVC structures are implemented and evaluated. A brief diagram of the experimental setup is presented in Fig. 23.

Remark 5 Since the simulation comparisons have been performed to compare the proposed WVC and other wave based approaches, in this experimental studies we only evaluate the performances of WVT and WVC as well as scaled WVC structures in bilateral teleoperation tasks.

5.3.1 WVT Structure

In the experiments with WVT structure, the wave impedance b is set to 0.1 in free motion and 1.2 in contact phantom experiment[1]. The velocity and the force tracking performances are illustrated in Fig. 24 (free motion) and 25 (in contact).

[1]Based on the free motion/contact environment and trial results. Different values can also be used in the experiment and cause slight changes of tracking performances.

It is clear from the illustrated experimental results that WVT structure can provide stable tracking performance in both experiments. However, significant fluctuation of the feedback force at the master side is noticeable even in free motion.

It is seen from Figs. 24 and 25 that stable tracking performances were achieved with WVT structure under time delay in communication channel in both free motion and contact experiments. From Fig. 24, it is noted that even for free motion there exists slight feedback force from the slave side, which is mainly caused by the bias terms in the force tracking of the WVT structure as seen in (13). And the velocity and position trackings show notable vibrations. When contact with environment, significant mismatches between master and slave in terms of velocity/position and force trackings are observed, which again reflects the fact that the bias terms as in conventional WVT structure lead to poor tracking performances.

5.3.2 WVC Structure

In this experiment study, the two parameters of energy reservoir α and β are set to 1, and the initial values of both energy reservoirs are set to $500J$.

The free motion experiment is conducted first, and the velocity and force tracking performances are recorded and shown in the Fig. 26. With the same setup, a contact experiment is performed to move the slave robot from free space into contact with the phantom. The tracking performances of this experiment are provided in Fig. 27. It can be seen that the tracking performances are stable and the slave robot tracks well the master's motion with slight time delay. The same is observed for the feedback force at the master side and the contact force of slave.

Table 2 Comparison of wave based methods

Method	Brief description	Tracking performance	Passivity condition
WVT	Traditional approach, transmits wave variable u_m and v_s which are constructed from the force and velocity information as: $u_m(t) = \frac{1}{\sqrt{2b}}(f_{md}(t) + b\dot{x}_m(t))$ and $v_s(t) = \frac{1}{\sqrt{2b}}(-f_s(t) + b\dot{x}_{sd}(t))$	$\dot{x}_{sd}(t) = \dot{x}_m(t-T) + \frac{1}{b}(f_{md}(t-T) - f_s(t))$ $f_{md}(t) = f_s(t-T) + b(\dot{x}_m(t) - \dot{x}_{sd}(t-T))$	Always passive if $b > 0$
Modified wave variable (MWV) base controller [35]	Different from the wave variable construction in WVT, the MWV approach changes the wave variable transformation by adding wave impedance α, thus the wave variables transmitted between master and slave have been changed as: $u_m(t) = f_{md}(t) + b\dot{x}_m(t)$ and $v_s(t) = -b^2 f_s(t) + \alpha\dot{x}_{sd}(t)$	$\dot{x}_{sd}(t) = \dot{x}_m(t-T) + \frac{1}{b}(f_{md}(t-T) - f_s(t))$ $f_{md}(t) = f_s(t-T) + b\dot{x}_m(t) - \frac{b}{\alpha}\dot{x}_{sd}(t-T)$	Passivity is achieved by properly selecting b and α
New wave based teleoperator [36]	In order to reduce the wave reflection and effect of environment, a new wave based teleoperator is designed with new outgoing wave variables as:$u_m(t) = \frac{1}{\sqrt{2b}}(f_s(t-T) + b\dot{x}_m(t))$ and $v_s(t) = \frac{1}{\sqrt{2b}}f_s(t)$	$\dot{x}_{sd}(t) = \dot{x}_m(t-T) + \frac{f_s(t-2T)}{b} - \frac{f_s(t)}{b}$ $f_{md}(t) = f_s(t-T) + b\dot{x}_m(t)$	Always passive if $b > 0$
Augmented wave variable with enhanced force feedback [37]	To improved the feedback force to the master, the augmented wave variable approach uses a wave variable terms at the master side, the wave variables u_m and v_s keeps the same as the WVT, but the received wave variables at the master side changes to: $v_m(t) = v_s(t-T) + \Delta v_a$, and $\Delta v_a = \frac{\lambda}{0.5s+\lambda}(\dot{x}_m(t) - \dot{x}_{sd}(t-T))$	$\dot{x}_{sd}(t) = \dot{x}_m(t-T) + \frac{1}{b}(f_{md}(t-T) - f_s(t))$ $f_{md}(t) \approx f_s(t-T)$	Passivity of the system can be guaranteed by tuning the λ of the low-pass filter
Augmented wave variable with improved position tracking [38]	Similar as in [37], but with wave variable terms at the slave side to improve the position tracking performance, thus the received wave variable at the slave side can be changed as: $u_s(t) = u_m(t-T) + \Delta u_a$, and $\Delta u_a = \frac{1}{\sqrt{2b}}\frac{\lambda}{s+\lambda}(-f_{md}(t-T) + f_s(t))$	$f_{md}(t) = f_s(t-T) + b\dot{x}_m(t) - \frac{b}{\alpha}\dot{x}_{sd}(t-T)$ $\dot{x}_{sd}(t) \approx \dot{x}_m(t-T)$	Passivity of the system can be guaranteed by tuning the λ of the low-pass filter

Table 2 (continued)

Method	Brief description	Tracking performance	Passivity condition
WVC	In order to improved both position and force tracking performance, two wave variable compensation terms are designed at both master and slave side, the energy reservoirs based regulators are designed to limit the wave variable compensation terms from passivity point of view.	$\dot{x}_{sd}(t) \approx \dot{x}_m(t-T)$ and $f_{md}(t) \approx f_s(t-T)$	Passivity can be achieved by tuning energy reservoir based regulator

In order to quantitatively evaluate the tracking performances, the root mean square error (RMSE) of the velocity and the force tracking for both free motion and in contact experiments of WVC and conventional WVT as in 5.3.1 are calculated as

$$RMSE_{velocity} = \sqrt{\frac{1}{n}\sum_{i=1}^{n}(\dot{x}_{sd}(i) - \dot{x}_m((i-1)))^2} \quad (45)$$

$$RMSE_{position} = \sqrt{\frac{1}{n}\sum_{i=1}^{n}(x_{sd}(i) - x_m((i-1)))^2} \quad (46)$$

$$RMSE_{force} = \sqrt{\frac{1}{n}\sum_{i=1}^{n}(f_{md}(i) - f_s((i-1)))^2} \quad (47)$$

The results of RMSE of the velocity and force tracking performances are given in Table 3. Compared with the WVT structure, the proposed WVC structure has reduced the RMSE of velocity and force trackings by 76.7% (velocity tracking in free motion),88.9% (position tracking in free motion), 91.1% (force tracking in free motion), 32.4% (velocity tracking in contact), 85.5%(position tracking in contact) and 93.8% (force tracking in contact) respectively. It is clear that the force tracking performances of the proposed WVC structure are far better than WVT structure; and the velocity and position tracking performances are also improved.

Remark 6 In real MIS implementation, the acceptable operation error is always task-specific and therefore varies according to different operations: e.g. for suturing task in beating heart mitral valve surgery, the mean error is $8 \pm 5mm$ [51]; for Unicondylar Knee Arthroplasty (UKA), the allowed tolerance is $2mm$ for position error [52]; while for thoracolumbar spine surgery, the pedicle screw placement has 1 mm translational margin of error [53]. Since force feedback has not been conducted in previous medical interventions, to the knowledge of the authors, there exists no study on acceptable force error for real MIS operation yet. In any sense, the operation errors are expected to be as low as possible. It should also be noted these results given in Table 3 may not present quantitative guidance to real implementations because of different system set-ups (e.g. operation constraints, tool lengths, etc.), but they do show qualitative indication on the advantage of our proposed WVC structure in practice.

5.3.3 Scaled WVC Structure

In the scaled WVC experiment, the master position command is scaled by k_p before sending to the slave and the force feedback information from the slave side is scaled by

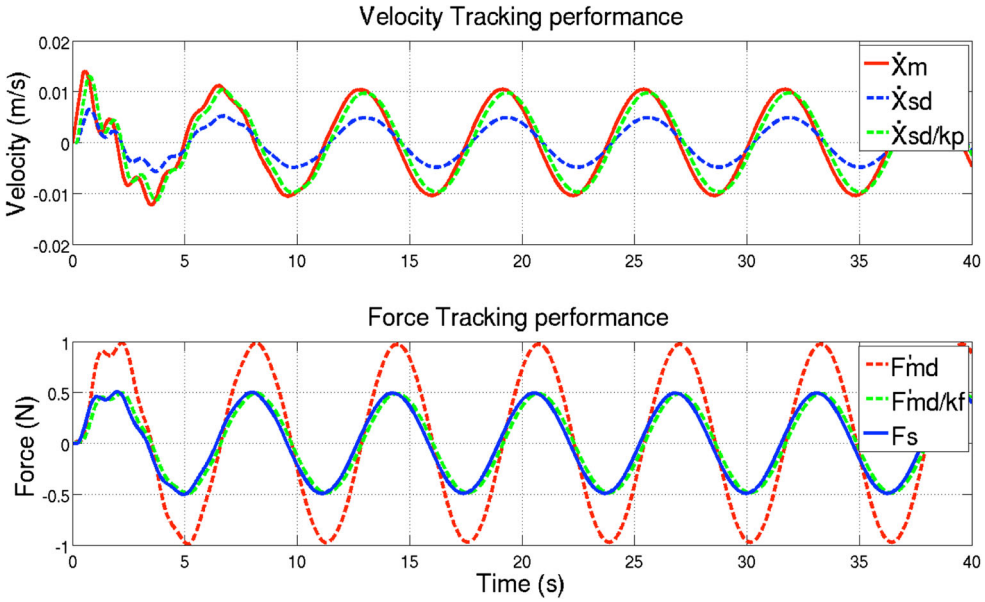

Fig. 20 Simulation results of ***scaled WVC*** based bilateral teleoperation ***(200ms)*** with $k_f = 2$ ***and*** $k_p = 0.5$

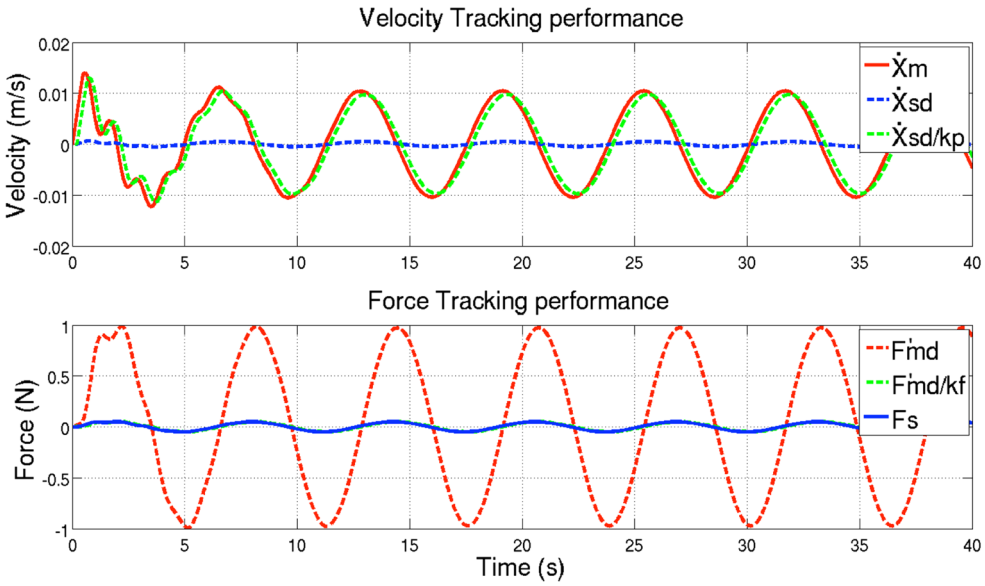

Fig. 21 Simulation results of ***scaled WVC*** based bilateral teleoperation ***(200ms)*** with $k_f = 20$ ***and*** $k_p = 0.05$

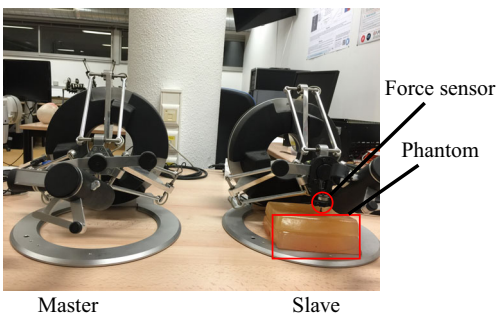

Fig. 22 Experiment platform using two Omega 7 robotic devices and force sensor

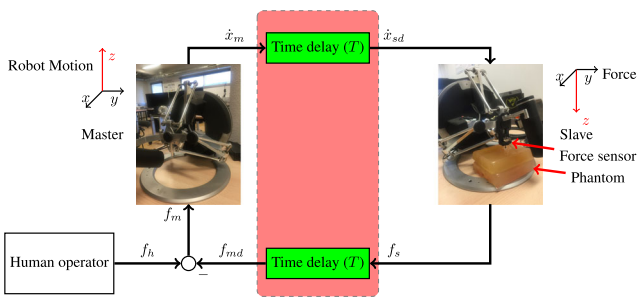

Fig. 23 Experiment system diagram

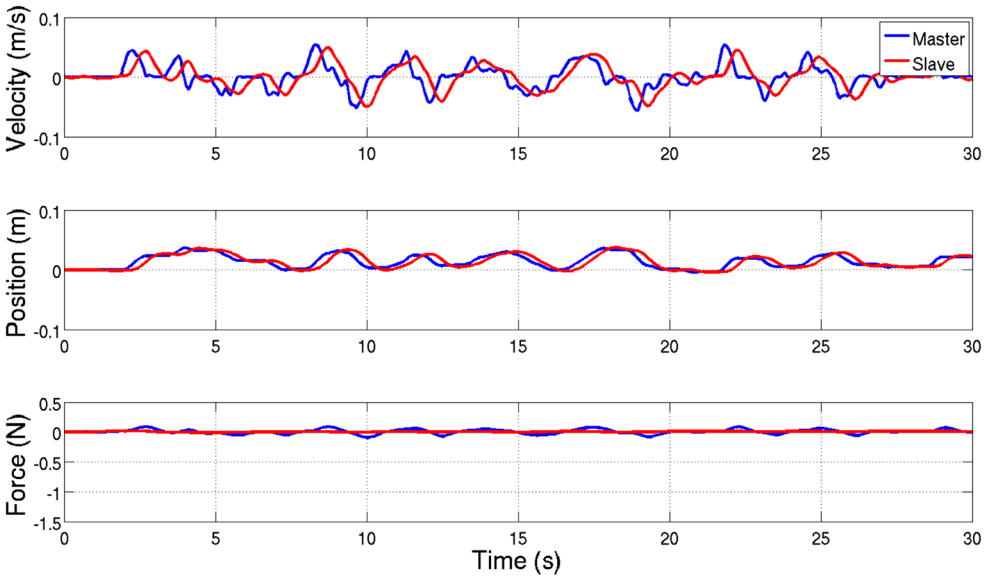

Fig. 24 Tracking performance of the ***WVT structure*** in free motion

k_f before rendering to the master. The experiments for both "free motion" and "in contact" situations run for 30 seconds with motion scale k_p and force scale k_f set to $k_p = 0.5$ and $k_f = 2.0$ respectively (which meets the passivity and transparency conditions as derived from Eqs. 33 and 42).

1. ***Free motion***: The velocity and force tracking performance are recorded and shown in Fig. 28. The slave velocity $\dot{x}_{sd}$ is scaled down by a factor k_p. The master desired force is scaled up with the scaling factor k_f, however, the scaled force tracking performance is hard to judge because the slave is moving in free space and the force sensor detects no contact force but only part of its own inertia and measurement noises.
2. ***In contact***: The operator moves the master and the slave robot follows the motion of the master to contact the phantom from free space for two times. The scaled and unscaled velocity and force tracking performances are provided in Fig. 29.

The statistic results of the achieved scales between master and slave's motion (velocity, position) and force during the 30 seconds' experiment duration are provided in Table 4. For each data set of the total 30000 samples ($30 \times 1k$), the motion and force scales are calculated and recorded respectively. Their average values are calculated as arithmetic mean of the recorded samples and the standard deviations are calculated based on the arithmetic mean

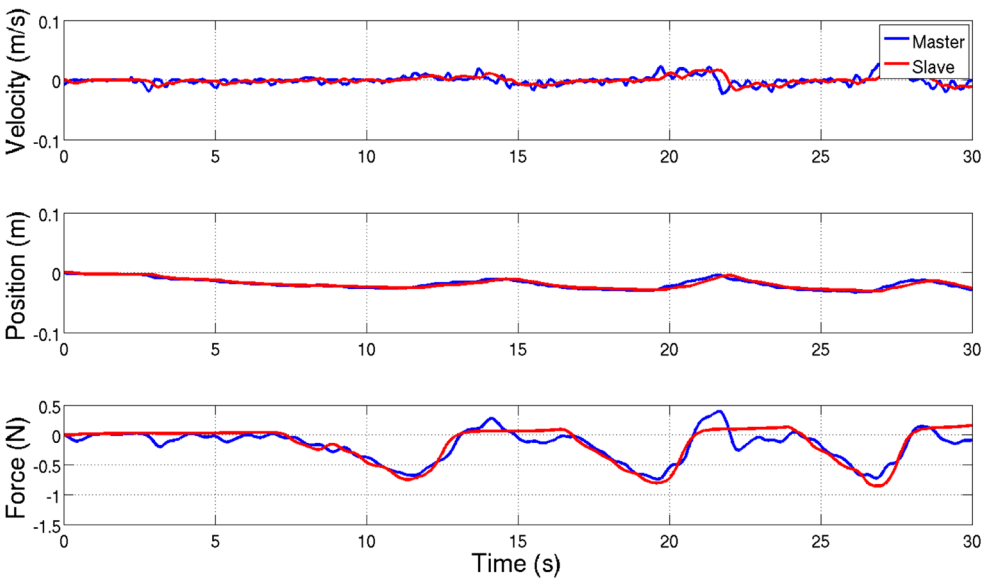

Fig. 25 Tracking performance of the ***WVT structure*** in contact with phantom

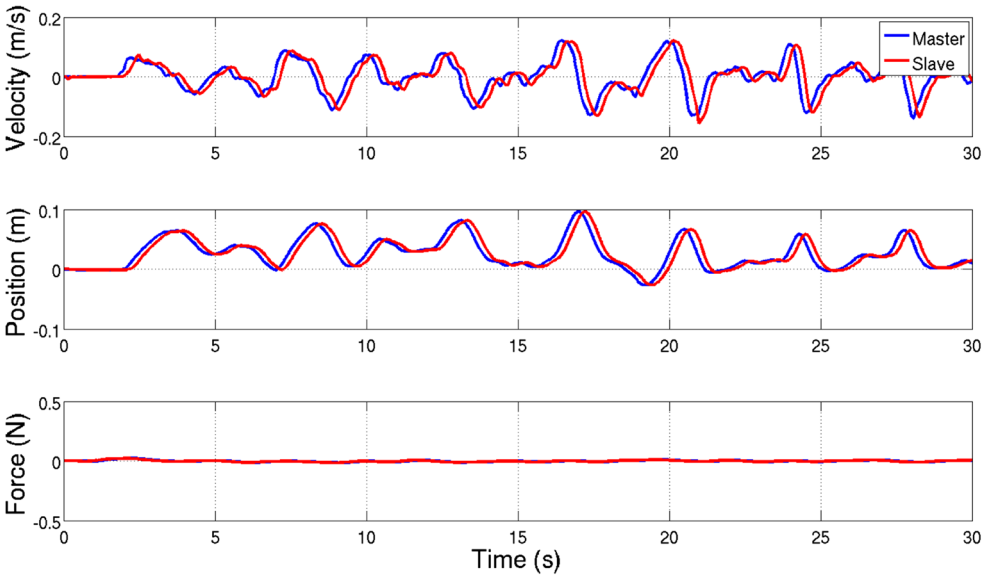

Fig. 26 Tracking performance of the ***WVC structure*** in free motion

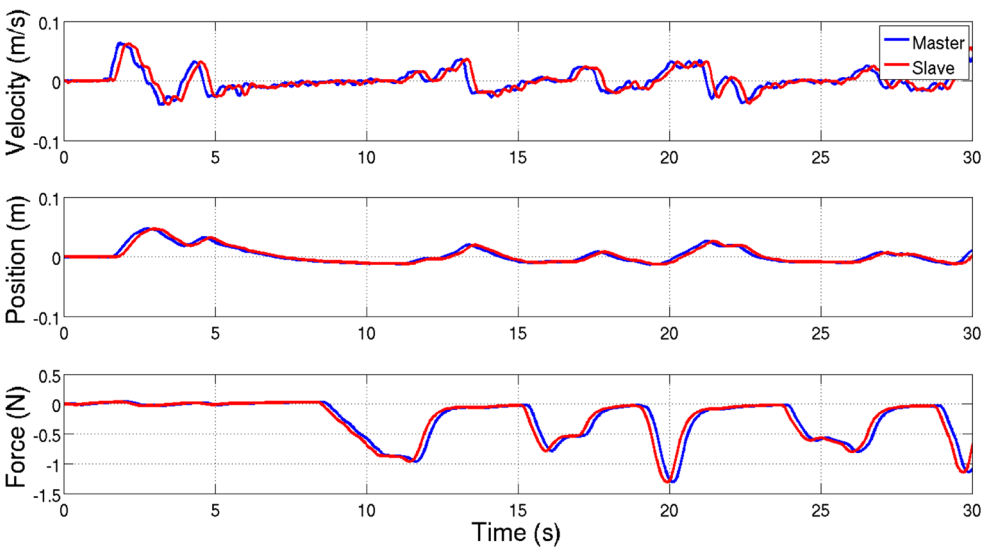

Fig. 27 Tracking performance of the ***WVC structure*** in contact with phantom

Table 3 RMSE of velocity, position and force tracking

		WVT	WVC
Free motion	Velocity (m/s)	0.0176	0.0041
	Position (mm)	14.3	1.6
	Force (N)	0.0688	0.0061
In contact	Velocity (m/s)	0.0207	0.0140
	Position (mm)	17.3	2.5
	Force (N)	0.3197	0.0199

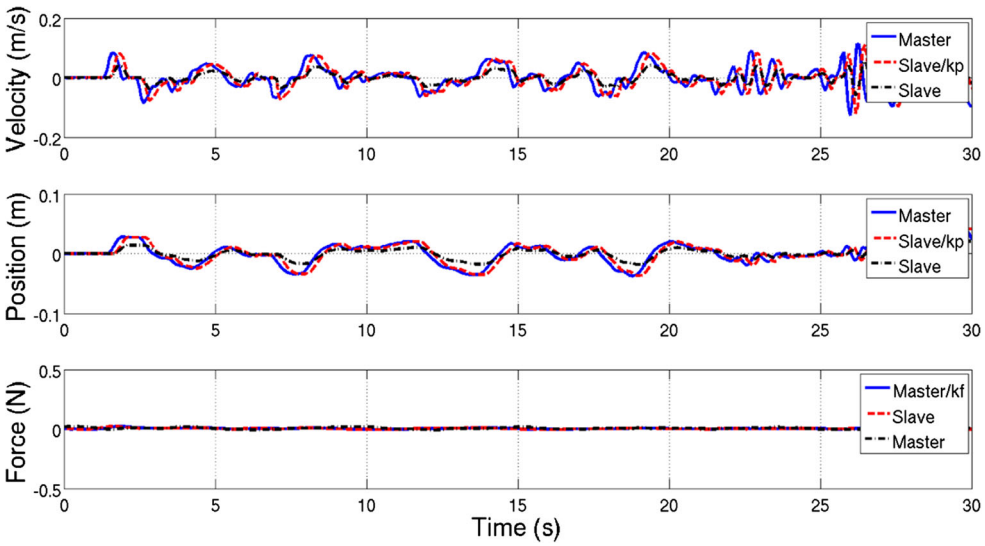

Fig. 28 Tracking performance of the ***scaled WVC structure*** in free motion ($k_p = 0.5$ and $k_f = 2.0$)

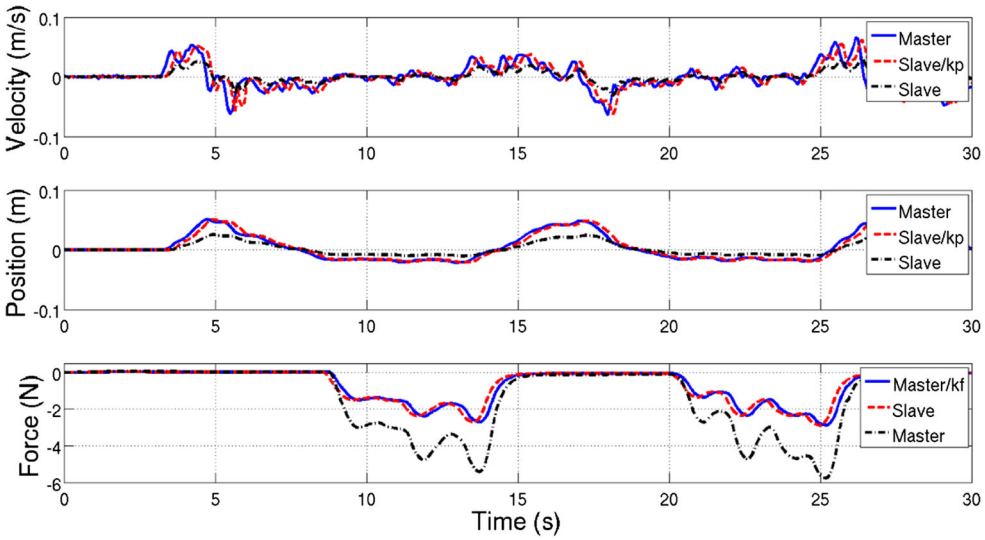

Fig. 29 Tracking performance of the ***scaled WVC structure*** in contact ($k_p = 0.5$ and $k_f = 2.0$)

Table 4 Analysis of experimentally achieved scales with WVC structure

		Designed	Avg.	Std (σ)
Free motion	Velocity	0.5	0.4956	0.0314
	Position	0.5	0.4926	0.0418
	Force	2.0	1.8941	0.1378
In contact	Velocity	0.5	0.5021	0.0832
	Position	0.5	0.4819	0.0529
	Force	2.0	1.9542	0.2135

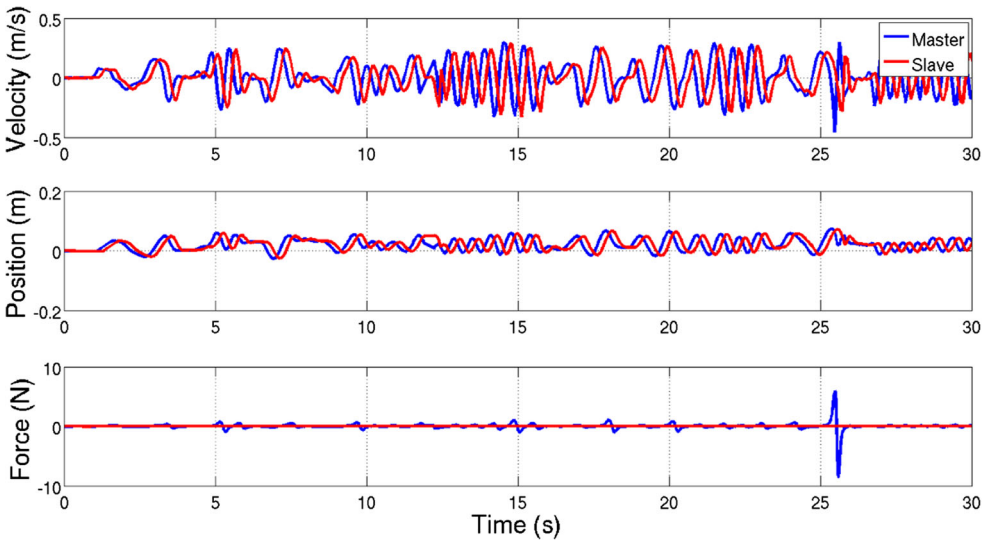

Fig. 30 Tracking performance of the ***WVC structure*** in free motion (energy reservoir $50J$)

and the recorded data. From this table, it is observed that achieved tracking scales through the experiments are very close to their designed scale values.

5.4 Discussions on Energy Reservoir Based Regulator

In the proposed WVC structure, there are three parameters of the energy reservoir that affect the system performance: α, β and its initial value. In the experimental studies, it is chosen that $\alpha = 1.0$, $\beta = 1.0$. According to the experimental tests, the major factor that affects the performance of WVC structure appears to be the initial value of the energy reservoirs $(E'_m(0), E'_s(0))$. In order to verify the influence of initial energy reservoir value on the WVC structure, two experiments in free motion have been performed to to simplify the situation and avoid potential disturbances of uncertainties when in contact with the environment.

The first free motion experiment is performed with the initial energy reservoir value of $50J$, the velocity and force tracking performance are recorded as in Fig. 30, and the according energy stored in the energy reservoirs is also provided in Fig. 31.

The second free motion experiment is performed with the initial energy reservoir value as $500J$, the velocity and force tracking performance are recorded in the Fig. 32, and the energy stored in the energy reservoirs is provided in Fig. 33.

From Fig. 30 for the first experiment, it is noted that the force feedback to the master rose rapidly at around 26s up to +6N and then dropped down to -8N. In Fig. 31, it can be

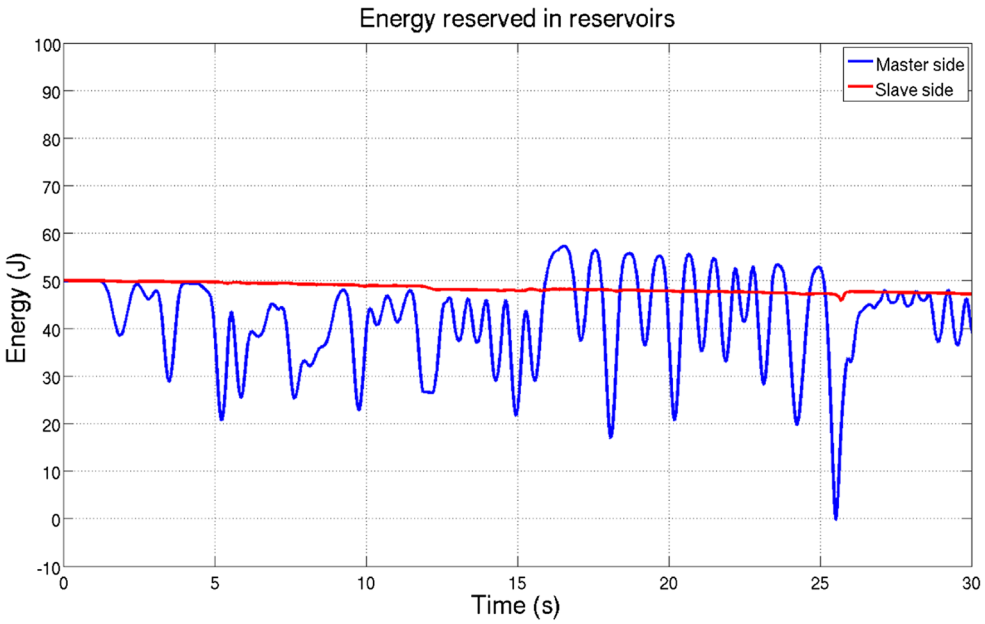

Fig. 31 Energy stored in the reservoirs of the ***WVC structure*** in free motion (energy reservoir $50J$)

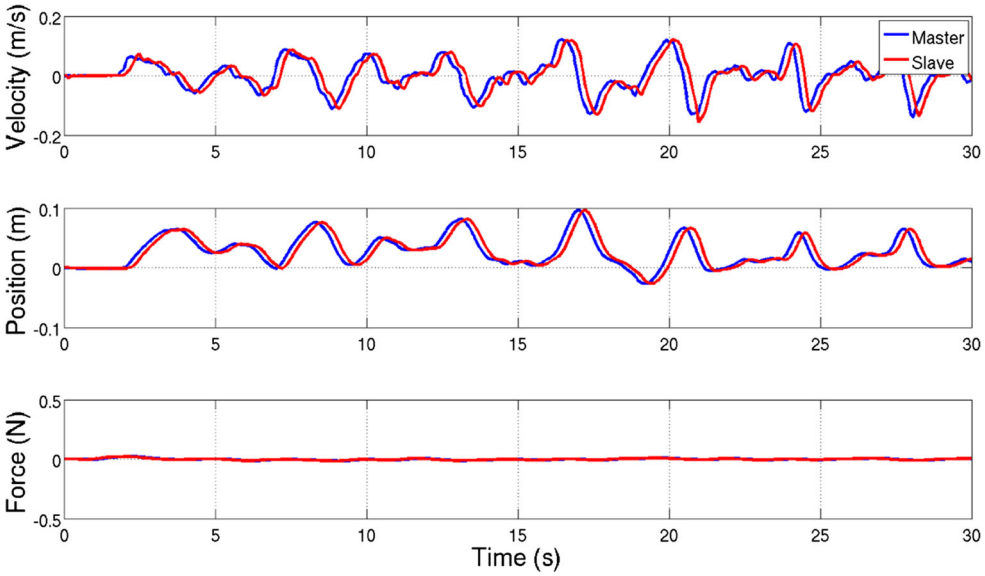

Fig. 32 Tracking performance of the ***WVC structure*** in free motion (energy reservoir $500J$)

seen that it corresponds to the sudden drop (close to 0) of stored energy in the energy reservoir on the slave side during the experiment.

With initial value of the energy reservoir increases to $500J$ as in the second experiment, enhanced feedback force and velocity tracking can be obtained as in Fig. 32 where all tracking performances are faithful and stable, and the energy stored in reservoirs shows no significant changes as seen in Fig. 33. It is observed that with the increased initial value of energy reservoir better tracking performance can be obtained, especially in term of smoothness. Also, it is interesting to see that with increased initial energy in the reservoirs, the system always remain stable ($E_s', E_m' > 0$). And even in cases of temporary drops in the stored energy, passivity can be retained as the stored energy is far from becoming negative and therefore the tolerance range for disturbances is increased.

On the contrary, the system can easily become unstable with lower initial energy reservoir in the first experiment because of non-passive behavior or too much wave variable compensation introduced into the bilateral teleoperation system at the beginning as lower initial energy leaves lower tolerance margin for disturbances, even if they are temporary.

Remark 7 The experimental studies were carried out along one axis. It is true that in surgical operations multiple DoFs are always needed for surgical tools' movement,

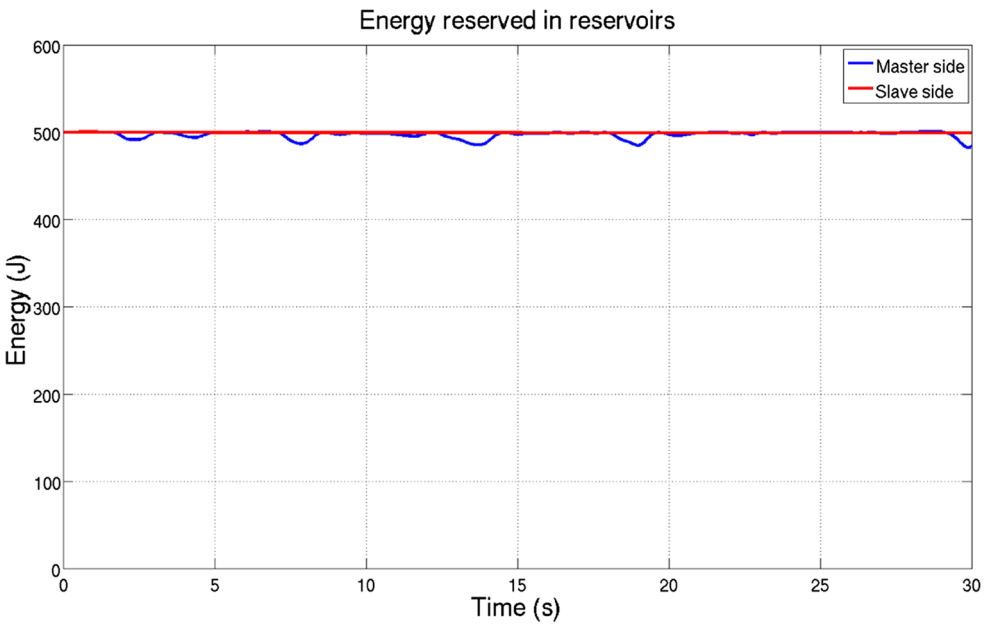

Fig. 33 Energy stored in the reservoirs of the ***WVC structure*** in free motion (energy reservoir $500J$)

but this is not necessarily the case for force reflection or interaction feedback with the environment (human tissue). From technical point of view, the motion control for each DoF of surgical robot can be separated from the other DoFs because of the fact that system set-up is usually well constructed and there is adequate pre-operative calibration time to obtain system kinematic and dynamic parameters with high enough accuracy to carry out inverse kinematics calculation or dynamics decoupling online without sacrificing motion control precision. Also, decentralized or decoupled motion control allows to pre-define control performance specifications especially for transient performance, which is extremely important for surgery safety. Therefore, we have evaluated our proposed haptic teleoperation method in 1-D, which appears to be also the common evaluation practice in bilateral teleoperation literature [39, 54–56] etc.

6 Conclusion

The classic wave variable transformation (WVT) is able to passiviate the communication channel with time delay in bilateral teleoperation, but can only provide biased tracking performance which are not sufficient for teleoperation tasks with high requirement due to its conservative nature. Driven by the need of higher transparency, a less conservative method is proposed in this work, named wave variable compensation (WVC) structure. The tracking performance of the WVC is improved by introducing wave variable compensation terms, with consideration of the passivity of the master and slave sides (including operator and environment). The *passivity* of the whole system is guaranteed by using energy reservoir based regulators. Further analysis of the energy reservoir based regulator in WVC is performed. To facilitate robotic-assisted surgery, scaled position/velocity and force tracking performance are also considered based on WVC structure. Through the passivity and transparency analysis, two conditions are derived to guarantee satisfactory scaled tracking performance. Both simulation and experimental studies have been carried out to verify the efficiency of the proposed WVC and scaled WVC approaches, and consistent conclusions are drawn based on the simulation and experiment results. Quantitative analysis of the experimental studies are provided to verify that enhanced tracking performance can be achieved to facilitate the bilateral teleoperation tasks, especially with high tracking performance requirements. The detailed analysis of energy reservoir based regulator is expected to benefit the utilization of such methods in later teleoperation applications. Future research may include integrating wave predictor approaches with the developed WVC structure to further improve velocity/position and force tracking performances, carrying out experimental evaluations with haptic feedback from multiple axes, and extending this work to handle asymmetric time-varying communication delay.

Acknowledgements This work was partially supported by Guangzhou Elite Project and National Natural Science Foundation of China (Grant 61803103).

References

1. Nguan, C., Miller, B., Patel, R., Luke, P.P., Schlachta, C.M.: Pre-clinical remote telesurgery trial of a da vinci telesurgery prototype. Int. J. Med. Rob. Comput. Assisted Surg. **4**(4), 304–309 (2008)
2. Panait, L., Akkary, E., Bell, R.L., Roberts, K.E., Dudrick, S.J., Duffy, A.J.: The role of haptic feedback in laparoscopic simulation training. J. Surg. Res. **156**(2), 312–316 (2009)
3. Tahmasebi, A.M., Hashtrudi-Zaad, K., Thompson, D., Abolmaesumi, P.: A framework for the design of a novel haptic-based medical training simulator. IEEE Trans. Inf. Technol. Biomed. **12**(5), 658–666 (2008)
4. Artigas, J., Hirzinger, G.: A brief history of dlr's space telerobotics and force-feedback teleoperation. Acta Polytech. Hung. **13**(1), 239–249 (2016)
5. Marturi, N., Rastegarpanah, A., Takahashi, C., Adjigble, M., Stolkin, R., Zurek, S., Kopicki, M., Talha, M., Kuo, J.A., Bekiroglu, Y.: Towards advanced robotic manipulation for nuclear decommissioning: a pilot study on tele-operation and autonomy. In: 2016 International Conference on Robotics and Automation for Humanitarian Applications (RAHA), pp. 1–8. IEEE (2016)
6. Murphy, R.R., Dreger, K.L., Newsome, S., Rodocker, J., Steimle, E., Kimura, T., Makabe, K., Matsuno, F., Tadokoro, S., Kon, K.: Use of remotely operated marine vehicles at minamisanriku and rikuzentakata Japan for disaster recovery. In: 2011 IEEE International Symposium on Safety, Security, and Rescue Robotics (SSRR), pp. 19–25. IEEE (2011)
7. Hokayem, P.F., Spong, M.W.: Bilateral teleoperation: an historical survey. Automatica **42**(12), 2035–2057 (2006)
8. Li, Z., Xia, Y., Sun, F.: Adaptive fuzzy control for multilateral cooperative teleoperation of multiple robotic manipulators under random Network-Induced delays. IEEE Trans. Fuzzy Systems **22**(2), 437–450 (2014)
9. Li, Z., Xia, Y., Wang, D., Zhai, D., Su, C.Y., Zhao, X.: Neural Network-Based control of networked trilateral teleoperation with geometrically unknown constraints. IEEE Trans. Cybernetics **46**(5), 1051–1064 (2016)
10. Bergeles, C., Yang, G.-Z.: From passive tool holders to microsurgeons: safer, smaller, smarter surgical robots. IEEE Trans. Biomed. Eng. **61**(5), 1565–1576 (2014)
11. Vitiello, V., Lee, S.-L., Cundy, T.P., Yang, G.-Z.: Emerging robotic platforms for minimally invasive surgery. IEEE Rev. Biomed. Eng. **6**, 111–126 (2013)
12. Taylor, R.H., Menciassi, A., Fichtinger, G., Fiorini, P., Dario, P.: Medical robotics and computer-integrated surgery. In: Springer Handbook of Robotics, pp. 1657–1684. Springer (2016)
13. Karas, C.S., Chiocca, E.A.: Neurosurgical robotics: a review of brain and spine applications. J. Robot. Surg. **1**(1), 39–43 (2007)
14. Burgner, J., Rucker, D.C., Gilbert, H.B., Swaney, P.J., Russell, P.T., Weaver, K.D., Webster, R.J.: A telerobotic system for transnasal surgery. IEEE/ASME Trans. Mechatron. **19**(3), 996–1006 (2014)

15. Mohr, F.W., Falk, V., Diegeler, A., Walther, T., Gummert, J.F., Bucerius, J., Jacobs, S., Autschbach, R.: Computer-enhanced robotic cardiac surgery: experience in 148 patients. J. Thorac. Cardiovasc. Surg. **121**(5), 842–853 (2001)
16. Okamura, A.M.: Methods for haptic feedback in teleoperated robot-assisted surgery. Industrial Robot: An International Journal **31**(6), 499–508 (2004)
17. Tavakoli, M.: Haptics for teleoperated surgical robotic systems. World Scientific Publishing Co. Inc., Singapore (2008)
18. Christopher, R., Nicholas, S., Robert, D.: The role of force feedback in surgery: analysis of blunt dissection. In: 10Th Symposium on Haptic Interface for Virtual Environment and Teleoperator Systems, vol. 1, pp. 18–125. IEEE Computer Society, Orlando (2002)
19. Meli, L., Pacchierotti, C., Prattichizzo, D.: Sensory subtraction in robot-assisted surgery: fingertip skin deformation feedback to ensure safety and improve transparency in bimanual haptic interaction. IEEE Trans. Biomed. Eng. **61**(4), 1318–1327 (2014)
20. ANSI-AAMI-ST79, Comprehensive guide to steam sterilization and sterility assurance in health care facilities. In: A1:2010, A2:2011, Association for the Advancement of Medical Instrumentation Arlington, VA
21. Konstantinova, J., Jiang, A., Althoefer, K., Dasgupta, P., Nanayakkara, T.: Implementation of tactile sensing for palpation in robot-assisted minimally invasive surgery: a review. IEEE Sens. J **14**(8), 2490–2501 (2014)
22. Hinterseer, P., Hirche, S., Chaudhuri, S., Steinbach, E., Buss, M.: Perception-based data reduction and transmission of haptic data in telepresence and teleaction systems. IEEE Trans. Signal Process. **56**(2), 588–597 (2008)
23. Kuschel, M., Kremer, P., Buss, M.: Passive haptic data-compression methods with perceptual coding for bilateral presence systems. IEEE Trans. Syst. Man Cybern. Part A Syst. Humans **39**(6), 1142–1151 (2009)
24. Kokkonis, G., Psannis, K., Roumeliotis, M.s., Kontogiannis, S.: A survey of transport protocols for haptic applications. In: 2012 16th Panhellenic Conference on Informatics (PCI), pp. 192–197. IEEE (2012)
25. Tortora, G., Dario, P., Menciassi, A.: Array of robots augmenting the kinematics of endocavitary surgery. IEEE/ASME Trans. Mechatron. **19**(6), 1821–1829 (2014)
26. Guo, J., Liu, C., Poignet, P.: Scaled position-force tracking for wireless teleoperation of miniaturized surgical robotic system. In: Engineering in Medicine and Biology Society (EMBC), 2014 36th Annual International Conference of the IEEE, pp. 361–365. IEEE (2014)
27. Shine, T.S.J., et al.: Specialized Operating Room (Chapter 13), Operation Room Design Manual, pp. 44–56. American Society of Anesthesiologists, Illinois, USA (2012)
28. Anderson, R.J., Spong, M.W.: Bilateral control of teleoperators with time delay. IEEE Trans. Autom. Control **34**(5), 494–501 (1989)
29. Niemeyer, G., Slotine, J.-J.: Stable adaptive teleoperation. IEEE J. Ocean. Eng. **16**(1), 152–162 (1991)
30. Baier, H., Schmidt, G.: Transparency and stability of bilateral kinesthetic teleoperation with time-delayed communication. J. Intell. Robot. Syst. **40**(1), 1–22 (2004)
31. Nuño, E., Basañez, L., Ortega, R.: Passivity-based control for bilateral teleoperation: a tutorial. Automatica **47**(3), 485–495 (2011)
32. Deng, Q.-W., Wei, Q., Li, Z.-X.: Analysis of absolute stability for time-delay teleoperation systems. Int. J. Autom. Comput. **4**(2), 203–207 (2007)
33. Franken, M., Stramigioli, S., Misra, S., Secchi, C., Macchelli, A.: Bilateral telemanipulation with time delays: a two-layer approach combining passivity and transparency. IEEE Trans. Robot. **27**(4), 741–756 (2011)
34. Yang, C., Wang, X., Li, Z., Li, Y., Su, C.-Y.: Teleoperation control based on combination of wave variable and neural networks. IEEE Trans. Syst. Man Cybern. Syst. **47**(8), 2125–2136 (2017)
35. Kawashima, K., Tadano, K., Wang, C., Sankaranarayanan, G., Hannaford, B.: Bilateral teleoperation with time delay using modified wave variable based controller. In: 2009. ICRA'09 IEEE International Conference on Robotics and Automation, pp. 4326-4331. IEEE (2009)
36. Bate, L., Cook, C.D., Li, Z.: Reducing wave-based teleoperator reflections for unknown environments. IEEE Trans. Ind. Electron. **2**(58), 392–397 (2011)
37. Ye, Y., Liu, P.X.: Improving haptic feedback fidelity in wave-variable-based teleoperation orientated to telemedical applications. IEEE Trans. Instrum. Meas. **58**(8), 2847–2855 (2009)
38. Ye, Y., Liu, P.X.: Improving trajectory tracking in wave-variable-based teleoperation. IEEE/ASME Trans. Mechatron. **15**(2), 321–326 (2010)
39. Li, H., Kawashima, K.: Achieving stable tracking in wave-variable-based teleoperation. IEEE/ASME Trans. Mechatron. **19**(5), 1574–1582 (2014)
40. Zhu, J., He, X., Gueaieb, W.: Trends in the control schemes for bilateral teleoperation with time delay. In: Kamel, M., Karray, F., Gueaieb, W., Khamis, A. (eds.) Autonomous and Intelligent Systems. Lecture Notes in Computer Science, vol. 6752. Springer, Berlin (2011)
41. Muradore, R., Fiorini, P.: A review of bilateral teleoperation algorithms. Acta Polytechnica Hungarica **13**(1), 191–208 (2016)
42. Ghavifekr, A.A., Ghiasi, A.R., Badamchizadeh, M.A.: Discrete-time control of bilateral teleoperation systems: a review. Robotica **36**(4), 552–569 (2018)
43. Guo, J., Liu, C., Poignet, P.: Stable and enhanced position-force tracking for bilateral teleoperation with time delay. In: Control Conference (ECC), 2015 European, pp. 1980-1985. IEEE (2015)
44. Lawrence, D.A.: Stability and transparency in bilateral teleoperation. IEEE Trans. Robot. Autom. **9**(5), 624–637 (1993)
45. Munir, S., Book, W.J.: Wave-based teleoperation with prediction. In: American Control Conference, 2001. Proceedings of the 2001, vol. 6, pp. 4605–4611. IEEE (2001)
46. Niemeyer, G.D.: Using wave variables in time delayed force reflecting teleoperation, Ph.D. thesis Massachusetts Institute of Technology (1996)
47. Ching, H., Book, W.J.: Internet-based bilateral teleoperation based on wave variable with adaptive predictor and direct drift control. J. Dyn. Syst. Meas. Control. **128**(1), 86–93 (2006)
48. Moreira, P., Zemiti, N., Liu, C., Poignet, P.: Viscoelastic model based force control for soft tissue interaction and its application in physiological motion compensation. Comput. Methods Prog. Biomed. **116**(2), 52–67 (2014)
49. Sanchez, L.A., Le, M., Liu, C., Zemiti, N., Poignet, P.: The impact of interaction model on stability and transparency in bilateral teleoperation for medical applications. In: 2012 IEEE International Conference on Robotics and Automation (ICRA), pp. 1607–1613. IEEE (2012)
50. Hashtrudi-Zaad, K., Salcudean, S.E.: Analysis of control architectures for teleoperation systems with impedance/admittance master and slave manipulators. Int. J. Robot. Res. **20**(6), 419–445 (2001)
51. Downing, S.W., Herzog, W.A., McLaughlin, J.S., Gilbert, T.P.: Beating-heart mitral valve surgery: preliminary model and methodology. J. Thorac. Cardiovasc. Surg. **123**(6), 1141–1146 (2002)
52. Mitsuishi, M.: Medical robot and master slave system for minimally invasive surgery. In: 2007. CME 2007. IEEE/ICME

International Conference on Complex Medical Engineering, pp. 8–13. IEEE (2007)
53. Puvanesarajah, V., Liauw, J.A., Lo, S.-f., Lina, I.A., Witham, T.F.: Techniques and accuracy of thoracolumbar pedicle screw placement. World J. Orthod. **5**(2), 112 (2014)
54. Tavakoli, M., Patel, R.V., Moallem, M.: Bilateral control of a teleoperator for soft tissue palpation: design and experiments. In: Proceedings 2006 IEEE International Conference on Robotics and Automation, 2006. ICRA 2006. pp. 3280-3285. IEEE (2006)
55. Christiansson, G.A., Van Der Helm, F.C.: The low-stiffness teleoperator slave—a trade-off between stability and performance. Int. J. Robot. Res. **26**(3), 287–299 (2007)
56. Colonnese, N., Okamura, A.M.: Analysis of effective impedance transmitted to the operator in position-exchange bilateral teleoperation. In: World Haptics Conference (WHC), pp. 328–333. IEEE (2017)
57. Moreira, P., Patil, S., Alterovitz, R., Misra, S.: Needle steering in biological tissue using ultrasound-based online curvature estimation. In: Proceedings of IEEE Int Conf Robot Autom, pp. 4368–4373. Hong Kong (2014)
58. Jian, B., Gao, W., Kacher, D., Nevo, E., Fetics, B., Lee, T.C., Jayender, J.: Kalman filter-based EM-optical sensor fusion for needle deflection estimation. Int. J. Comput. Assist. Radiol. Surg. **13**(4), 573–583 (2018)

Jing Guo is currently a lecturer working with School of Automation, Guangdong University of Technology, China. He was research fellow at National University of Singapore (NUS). He obtained his Ph.D degree from University of Montpelier, France. During his Ph.D study, he worked at LIRMM, a joint research center between University of Montpellier and the National Center for Scientific Research (CNRS). He received his bachelor and master degree both from Guangdong University of Technology in 2009 and 2012 respectively. His research interests include robotic control, haptic bilateral teleoperation, and machine learning.

Chao Liu received his Ph.D. degree in Electrical & Electronic Engineering from Nanyang Technological University, Singapore in 2006. He is currently Senior Research Scientist with LIRMM, CNRS (French National Center for Scientific Research). He has been principle investigator and participant in several French national and European projects. He is a review panelist for French National Research Agency (ANR) and Swiss National Science Foundation (SNSF). His research interests include surgical robotics, teleoperation, haptics, control theory/system, and computer vision.

Philippe Poignet is currently Director of LIRMM, CNRS and Full Professor at the University of Montpellier. His research interests include robot identification, nonlinear control and the applications to medical robotics. He has been involved as scientific leader in several national and European projects (FP6, FP7). He is co-organizer of the European Summer Schools in Surgical Robotics since 2003. He is also co-leader of the French national working group (GDR) on Medical Robotics.